RL-TR-91-164
Final Technical Report
July 1991

HYBRID ELECTRO-OPTIC PROCESSOR

COLSA, Inc.

Stephen T. Welstead (COLSA)
Michael J. Ward, 1Lt, USAF (Rome Laboratory)

APPROVED FOR PUBLIC RELEASE; DISTRIBUTION UNLIMITED.

Rome Laboratory
Air Force Systems Command
Griffiss Air Force Base, NY 13441-5700

This report has been reviewed by the Rome Laboratory Public Affairs Office (PA) and is releasable to the National Technical Information Service (NTIS). At NTIS it will be releasable to the general public, including foreign nations.

RL-TR-91-164 has been reviewed and is approved for publication.

APPROVED:

MICHAEL J. WARD, 1/LT, USAF
Project Engineer

FOR THE COMMANDER:

DR. DONALD W. HANSON
Acting Director
Surveillance & Photonics Directorate

If your address has changed or if you wish to be removed from the Rome Laboratory mailing list, or if the addressee is no longer employed by your organization, please notify RL(OCPA) Griffiss AFB NY 13441-5700. This will assist us in maintaining a current mailing list.

Do not return copies of this report unless contractual obligations or notices on a specific document require that it be returned.

REPORT DOCUMENTATION PAGE

Form Approved
OMB No. 0704-0188

1. AGENCY USE ONLY (Leave Blank)	2. REPORT DATE	3. REPORT TYPE AND DATES COVERED
	July 1991	Final Sep 88 - Sep 89

4. TITLE AND SUBTITLE
HYBRID ELECTRO-OPTIC PROCESSOR

5. FUNDING NUMBERS
C - F30602-88-D-0027
Task - P-8-0006
PE - 62702F
PR - 4600
TA - P1
WU - P1

6. AUTHOR(S)
Stephen T. Welstead, Michael J. Ward, 1/Lt, USAF

7. PERFORMING ORGANIZATION NAME(S) AND ADDRESS(ES)
COLSA, Inc.
6727 Odyessy Drive
Huntsville AL 35806

8. PERFORMING ORGANIZATION REPORT NUMBER

9. SPONSORING/MONITORING AGENCY NAME(S) AND ADDRESS(ES)
Rome Laboratory (OCPA)
Griffiss AFB NY 13441-5700

10. SPONSORING/MONITORING AGENCY REPORT NUMBER
RL-TR-91-164

11. SUPPLEMENTARY NOTES
Rome Laboratory Project Engineer: Michael J. Ward, 1/Lt, USAF/OCPA/(315) 330-2944
Rome Laboratory (formerly Rome Air Development Center/RADC)

12a. DISTRIBUTION/AVAILABILITY STATEMENT
Approved for public release; distribution unlimited.

12b. DISTRIBUTION CODE

13. ABSTRACT (Maximum 200 words)

This report describes the design of a hybrid electro-optic processor to perform adaptive interference cancellation in radar systems. The processor is designed to process wideband interference signals as well as multipath copies of these signals. The optical components in the processor include acousto-optic cells used as delay lines, a charge coupled device linear detector array, and a transmissive liquid crystal display spatial light modulator. The spatial light modulator is driven by an electronic microprocessor. A new way of achieving improved dynamic range for such a spatial light modulator is reported. Included in this report is a discussion of the design, partial fabrication in the laboratory, and partial testing of the hybrid electro-optic processor. A follow on effort is planned to complete the construction and testing of the processor. The work described in this report is the combined effort of RADC in-house project 4600P103 and Contract F30602-88-D-0027.

14. SUBJECT TERMS	15. NUMBER OF PAGES
Optical Processing, Adaptive Nulling, Spatial Light Modulator	48
	16. PRICE CODE

17. SECURITY CLASSIFICATION OF REPORT	18. SECURITY CLASSIFICATION OF THIS PAGE	19. SECURITY CLASSIFICATION OF ABSTRACT	20. LIMITATION OF ABSTRACT
UNCLASSIFIED	UNCLASSIFIED	UNCLASSIFIED	SAR

CONTENTS

LIST OF FIGURES

1. INTRODUCTION

This report describes the design and initial implementation of an electro-optic processor to perform sidelobe cancellation in radar systems. The work described here is the product of Expert in Science and Engineering contract F30602-88D-0027 and Rome Laboratory In-House project 4600P103. All work was performed at the Photonics Center of the Rome Laboratory, Griffiss Air Force Base, NY during the period of 13 SEP 88 to 30 SEP 89. The authors are indebted to the following personnel of the Rome Laboratory for their assistance: Dr. George Brost, Mr. Wesley Foor, and 1LT Edward Toughlian. The authors would also like to thank Mr. Andrew Pirich, Chief of the Analog Optical and Lightwave Signal Processing Branch, for providing needed encouragement and direction during the project.

The processor is designed to process jammer signals with a bandwidth up to 5 MHz at base-band, and multipath signals with delays up to 5 μsec. The preliminary design discussed here is configured for single channel (i.e., single jammer) processing, however, future plans call for a four channel system. This report includes a discussion of the design, partial fabrication, and preliminary testing of the hybrid electro-optic processor. A follow-on effort is planned to complete the construction and testing of the processor.

2. SYSTEM DESIGN

2.1. Background on the problem and the algorithm

The signal processing application addressed here is adaptive noise cancellation. The problem of implementing iterative algorithms to solve the noise/jammer cancellation problem has been looked at extensively in [1]. The algorithm we use here is an adaptive version of the steepest descent algorithm. We briefly consider here the application problem and the algorithm. For more details, see [1].

A main antenna receives both the signal of interest, s(t), and a noise signal n(t) whose exact characteristics are unknown. The total signal received at the main antenna is thus

$$d(t) = s(t) + n(t).$$

The problem is to construct a signal y(t) which is an estimate of n(t), so that the signal e(t), defined by

$$e(t) = d(t) - y(t)$$

is approximately equal to s(t).

The information that is available to construct y(t) comes from an omni-directional side antenna. We will use just one such antenna input in our architecture, although, in practice, several are used. The assumption is that the main antenna noise n(t) is a combination of different delayed versions of the signal $n_1(t)$ received by the side antenna. It is also assumed that s(t) and $n_1(t)$ are uncorrelated. Thus, we attempt to construct y(t) in the form

$$y(t) = \sum_{i=1}^{M} w_i \, n_1(t - (i-1)\,\Delta t). \qquad (2.1)$$

Here, Δt is the discrete time delay increment. The one dimensional vector

$$\underline{w} = (w_1,\ldots,w_M)$$

is called the weight vector. It is assumed that this vector changes slowly in time, compared to the signal modulation. We are interested, however, in having the algorithm adapt to changes in the weights over time.

The weight vector is to be chosen so as to minimize the energy of e(t). In theory, this energy is supposed to be minimized over all time. However, in a practical adaptive formulation of this problem, we must settle for minimization over a finite time interval from T - τ to the current time T, for some fixed τ. The minimization problem leads to a linear equation involving a covariance matrix. Iterative methods can be used to solve this equation. We choose an adaptive version of the steepest descent algorithm that is amenable to optical implementation. The adaptive version of this algorithm can be written in the form

$$w_i^{(N+1)} = w_i^{(N)} + a_N \int_{N\tau}^{(N+1)\tau} (d(t) - y^{(N)}(t))\, n_1(t - (i-1)\Delta t)\, dt \qquad (2.2)$$

$$i = 1,\ldots M.$$

Here, $w_i^{(N)}$ is the i^{th} component of the N^{th} iterate of the weight vector, $y^{(N)}(t)$ is the signal given by (2.1) with $w_i^{(N)}$ in place of w_i, and a_N is the scalar stepsize used to control convergence speed. The stepsize can either be fixed or can be made to vary dynamically with the iterations. In Section 4 we consider how this stepsize may be varied

in our system.

The algorithm (2.2) is what is implemented in the hybrid electro-optical processor. The architecture is presented in the next section. It should be pointed out that (2.2) differs, due to the time integration in the second term on the right, from the least mean square (LMS) algorithm implemented on many signal processor architectures.

2.2. The system architecture

The system architecture architecture for the electro-optic processor can be thought of as consisting of two optical subsystems connected by a microcomputer in a feedback loop, as shown in the block diagram of figure 2.2.1. The first optical subsystem, detailed in figure 2.2.2, forms updates to the weight vector. The second optical subsystem, as shown in figure 2.2.3, uses a spatial light modulator (SLM) to recombine the weight vector with delayed versions of the side signal to form the estimated noise signal y(t). Our earliest version of the system design incorporated a liquid crystal television (LCTV) display as a spatial light modulator. The complete electro-optic architecture with the LCTV is shown in figure 2.2.4.

The weight update vector is the vector whose i^{th} component is given by the integral in (2.2). These vector components are formed optically in parallel, using an acousto-optic (A/O) cell as a tapped delay line (as in [2]), and a charge coupled device (CCD) linear array to perform the time integration. The weight vector changes relatively slowly in time (compared to the signal modulation rates), so it is feasible to collect this information with a CCD array and then send it to the microcomputer via an analog to digital (A/D) converter.

The microcomputer performs the iteration step, forming the new weight vector by adding the weight update vector to the previously stored weight vector. The ability to retain previous weight information without degradation is an important advantage of this digital part of the system, as opposed to an all analog system. The microcomputer also uses weight update information to make an intelligent decision for computing the optimum value for the stepsize a_N on each iteration, as will be discussed in Section 4. Finally, and most significantly, the microcomputer is used to form the video output containing the special weight pattern information that will be displayed on the SLM.

A collimated HeNe beam illuminates the SLM. Light passing through the SLM is summed vertically by a cylindrical lens, resulting in a one dimensional spatially modulated beam which, as described in the next section, represents the weight vector. The estimated noise signal y(t) is formed by using an A/O cell to combine this weight vector with delayed versions of $n_1(t)$ and spatially summing the result with a spherical lens.

In the next section, we discuss the unique way in which the two dimensional SLM display is used as an improved dynamic range one dimensional SLM to represent the weight vector.

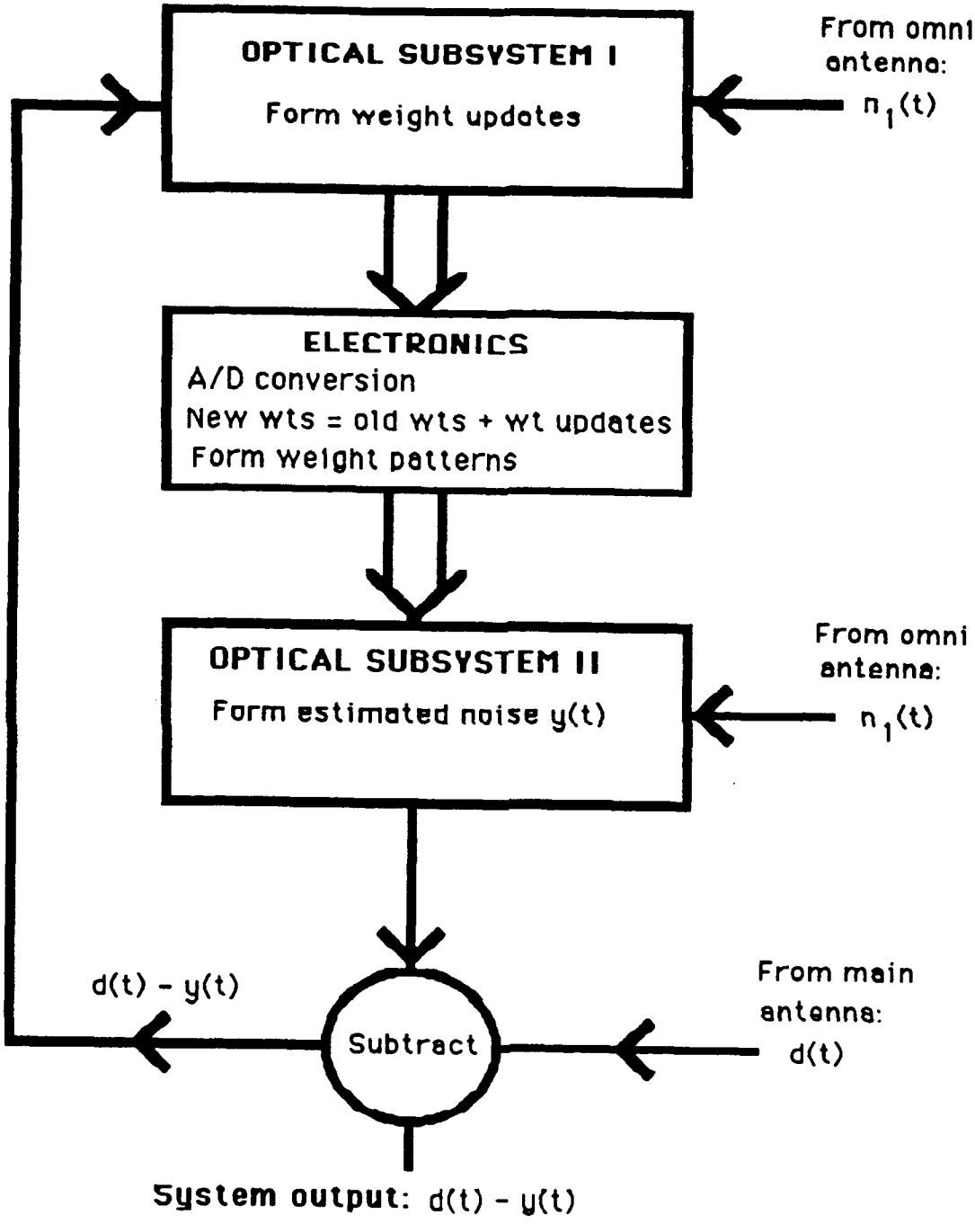

Figure 2.2.1 Block diagram of the system

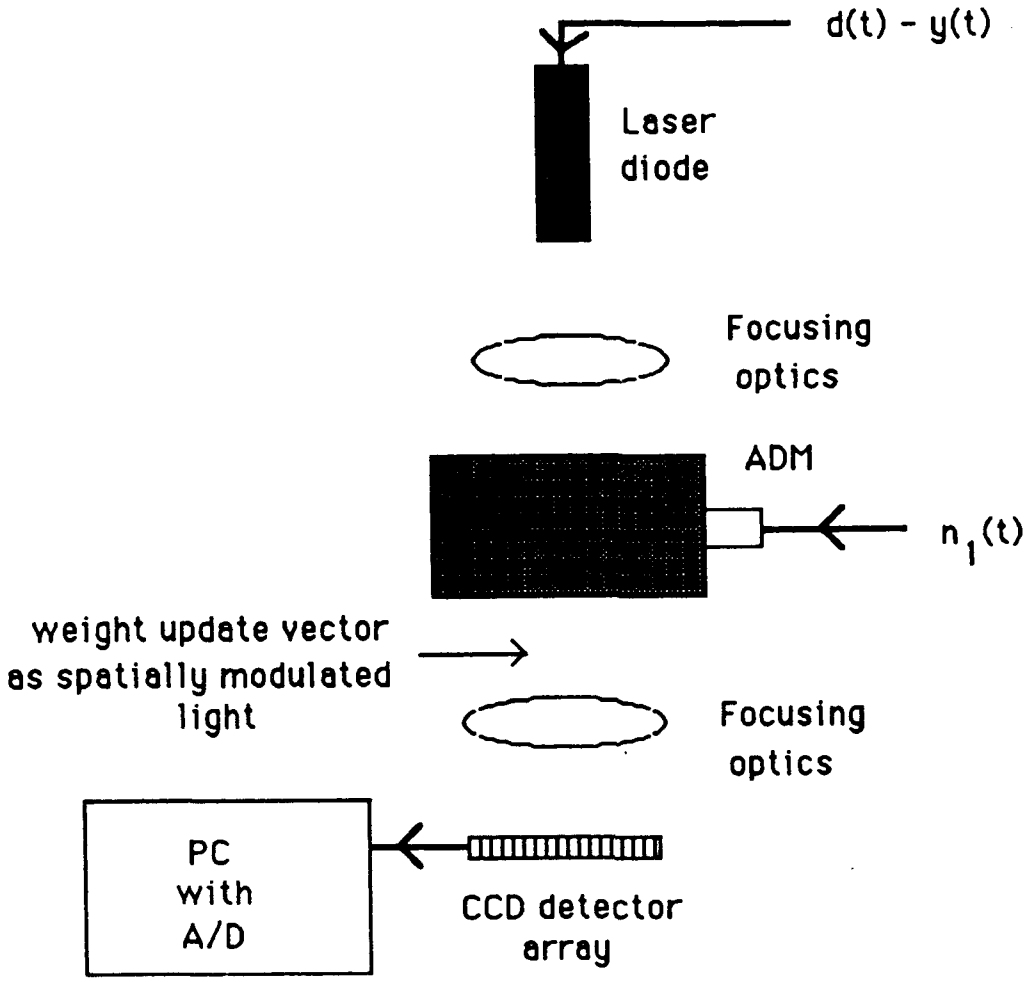

Figure 2.2.2 Optical subsystem I

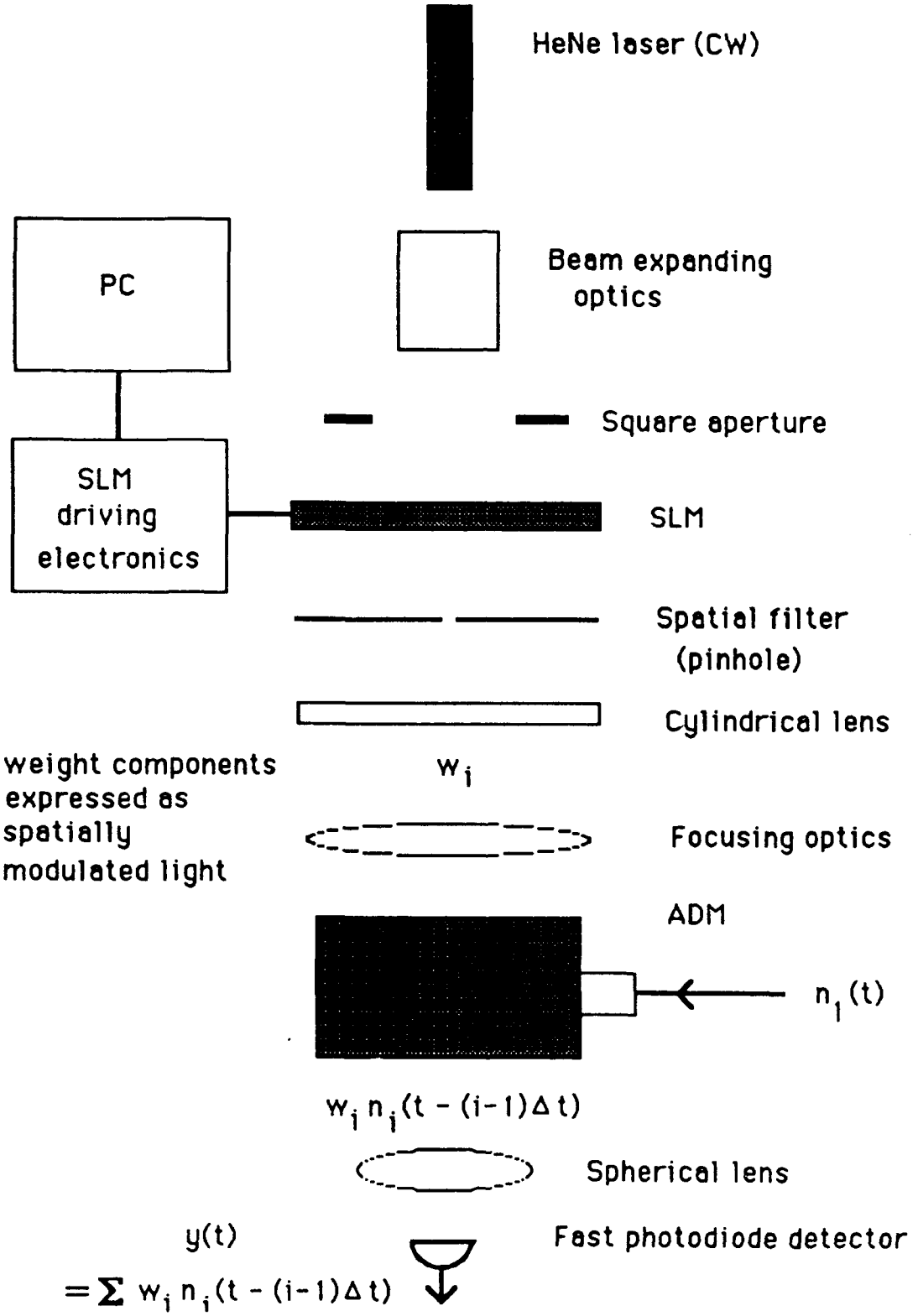

Figure 2.2.3 Optical subsystem II

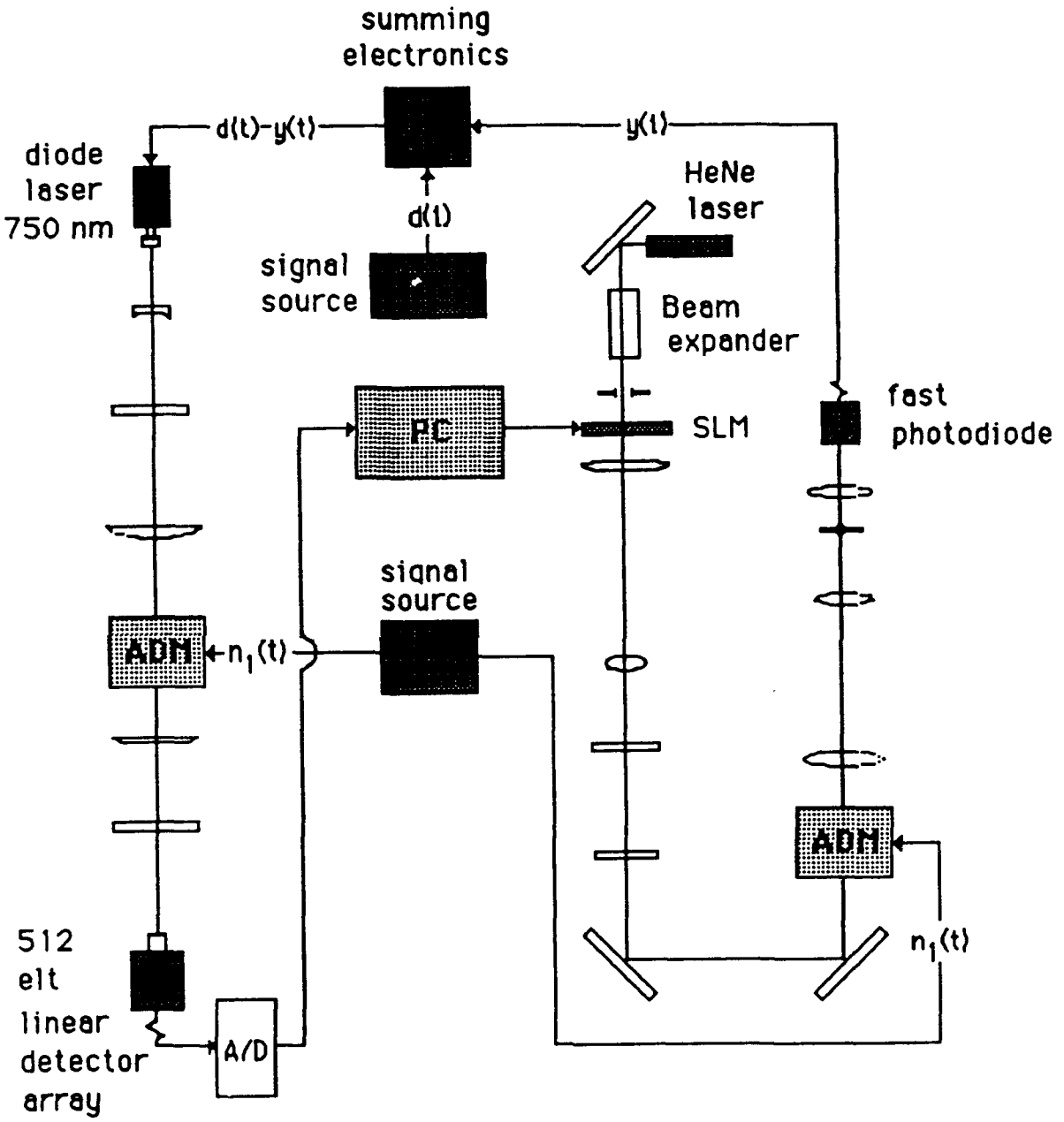

Figure 2.2.4 The complete electro-optic architecture

2.3. The LCTV as a spatial light modulator

The use of a LCTV as a two dimensional SLM has previously been considered by other investigators[4]. These researchers were primarily interested in the device as an inexpensive SLM for pattern recognition and image processing applications. The reported low dynamic range and number of gray scales were viewed as undesirable but tolerable limitations. The LCTV could replace SLM's which cost two orders of magnitude more in some of these applications.

For our purposes, we don't need two dimensions to represent the weight vector, but we do need much more numerical accuracy (ie., number of gray scales) than what is afforded by the device at the pixel level. Our experimental results discussed below indicate that, practically, we are limited to just the "on" and "off" states at each pixel. To overcome this, we use multiple numbers of pixels to represent different numeric values.

Specifically, we do the following to represent the weight vector as a pattern on the LCTV screen. The horizontal position across the screen corresponds to the particular component. The second screen dimension, namely the vertical direction, is used to represent the numerical value for each component. For example, if there are 100 total weight components, then the value for w_{50} is located halfway across the screen. A simple addressing scheme in the microcomputer can be used to translate component number into horizontal position on the screen (some consideration must be given, however, to the fact that the pixel grid structure of the LCTV does not correspond exactly to the pixel layout of the computer monitor). To represent the numerical value of this component, we simply turn "on" a number of vertical pixels that is proportional to the value. (For the purposes of our application problem, it is sufficient to consider weight values between 0 and 1 only.) This screen pattern is generated in the microcomputer and shipped to the LCTV using the LCTV's normal driving electronics.

The LCTV we use is an inexpensive commercially available device. Following the researchers mentioned above, we have modified the device by replacing the polarizing sheets with optical quality polarizers, and positioning the display in an upright manner so that it operates in a transmissive mode. The TV comes with a jack for video input, so that it can receive, for example, a video signal directly from the microcomputer.

The LCTV display is illuminated from behind by a collimated HeNe beam. The amount of light transmitted through a vertical column corresponding to a single weight component is then proportional to the numerical value of that component. This light is then summed in the vertical direction by a cylindrical lens. The result in the focal plane of this lens is a horizontal strip of light with spatial modulations corresponding to the values of the weight components. This concept is illustrated in Figure 2.3.1.

Figure 2.3.1 shows the LCTV illuminated by the collimated HeNe beam, a cylindrical lens summing in the vertical direction the output from the LCTV, and the spatially modulated

strip of light focused onto a linear detector array. This is the setup used to carry out the experiment described in the next section. The detector array is used for measurement purposes only in this experiment. In the system architecture shown in Figure 2.2.4, this detector is not present, and the output of the cylindrical lens is focused onto an A/O cell.

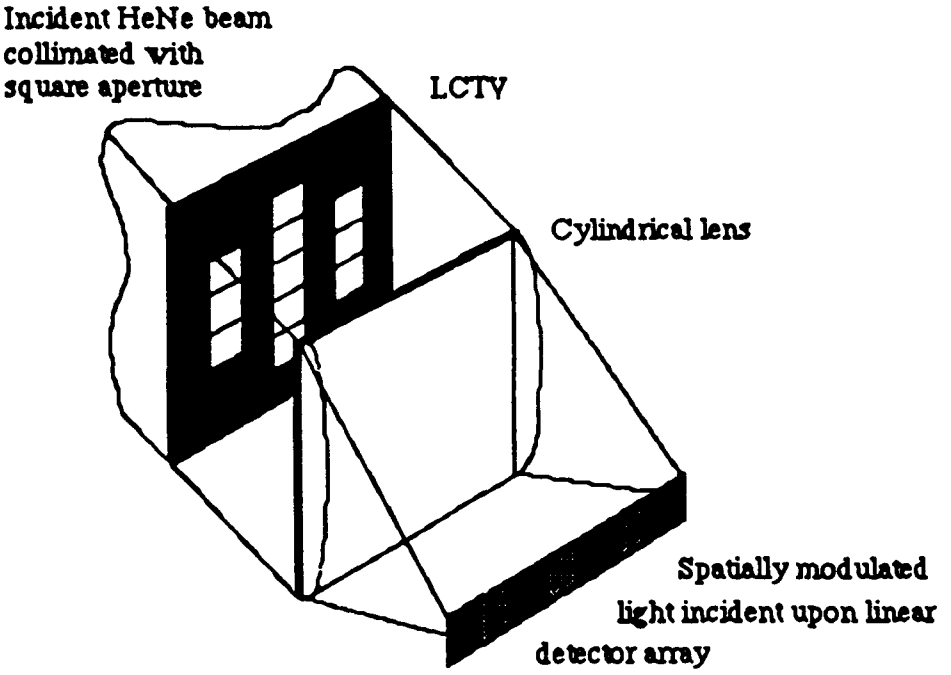

Figure 2.3.1 Experimental setup of the LCTV as a one dimensional SLM

In this way, we hope to achieve at least 100 gray levels for representing the weight values. Preliminary experimental results reported below show that 24 gray levels are easily achieved in this manner using only the "on"-"off" gray levels of the pixels and a coarse translation scheme for converting numbers to pixel patterns (ie., increments of 5 LCTV pixels at a time were used). We hope to improve this figure by introducing a finer translation scheme and perhaps making use of the intermediate gray scale available at the pixel level. A modification of the drive electronics of the TV may also help to improve dynamic range.

2.3.1 An Example

Figures 2.3.2 (a) - (b) illustrate this use of the LCTV as a one dimensional SLM. The sample weight pattern shown in Figure 2.3.2 (a) was generated by the microcomputer in CGA graphics mode (a total of 320 horizontal pixels and 200 vertical pixels for the entire computer monitor screen). The large center pattern is an area of 8X84 "on" pixels, while the two smaller patterns are areas of 8X28 "on" pixels. These are pixel numbers on the computer monitor screen. The LCTV has a total of 162 horizontal pixels and 149 vertical pixels for its entire screen [3], and so the pixel numbers for it will be less. The relative size of the larger pattern to the smaller ones is thus 3:1.

The light transmitted through the "on" pixels was summed in the vertical direction by the cylindrical lens and focused onto the linear detector array, as shown in Figure 2.3.1. Figure 2.3.2 (b) shows the oscilloscope trace of the detector output. One can see that the height of the large peak is very nearly 3 times the height of the smaller peaks. We are thus obtaining one dimensional spatial light modulation from the LCTV.

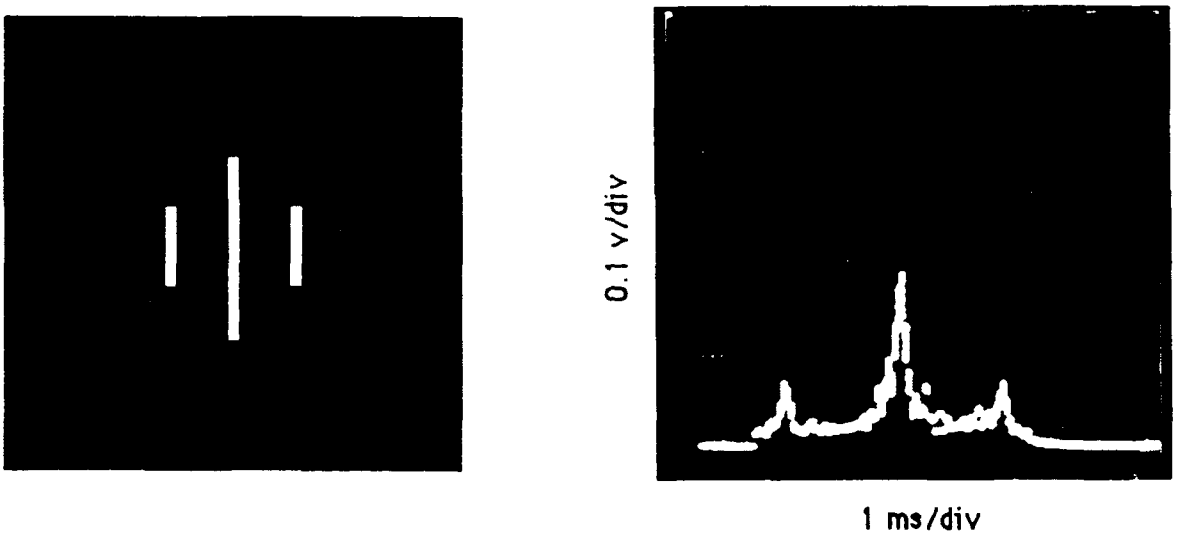

(a) The weight pattern on the computer screen (b) Oscilloscope trace of detector output

Figure 2.3.2 Experimental results

2.3.2 Spatial filtering

Close examination of figure 2.3.2 (b) shows that there is a positive level of light between the peaks. This light is undesirable, since it occurs in an area where the weight vector component values should be zero. It is suspected that at least some of this light is coming from leakage between the pixels. This light occurs at a high spatial frequency in the two dimensional plane of the LCTV display. The corresponding light in the Fourier transform plane would thus be relatively far removed from the origin. Following the suggestion of other investigators [4], we tested the incorporation of a spatial filter in the system to remove this high frequency light leakage.

Figures 2.3.3 (a) and (b) show the results of this test, using the same weight pattern of figure 2.3.2 (a). The spatial filter consisted of a pinhole located in the center of a piece of opaque material. Figure 2.3.3 (a) shows the digital oscilloscope trace of the unfiltered optical signal (this corresponds to the analog oscilloscope trace shown in figure 2.3.2 (b)). Figure 2.3.3 (b) shows the filtered optical signal, using a 0.0292 inch pinhole filter. One can see that the light leakage between peaks has been largely eliminated, with no degradation of the main optical signal.

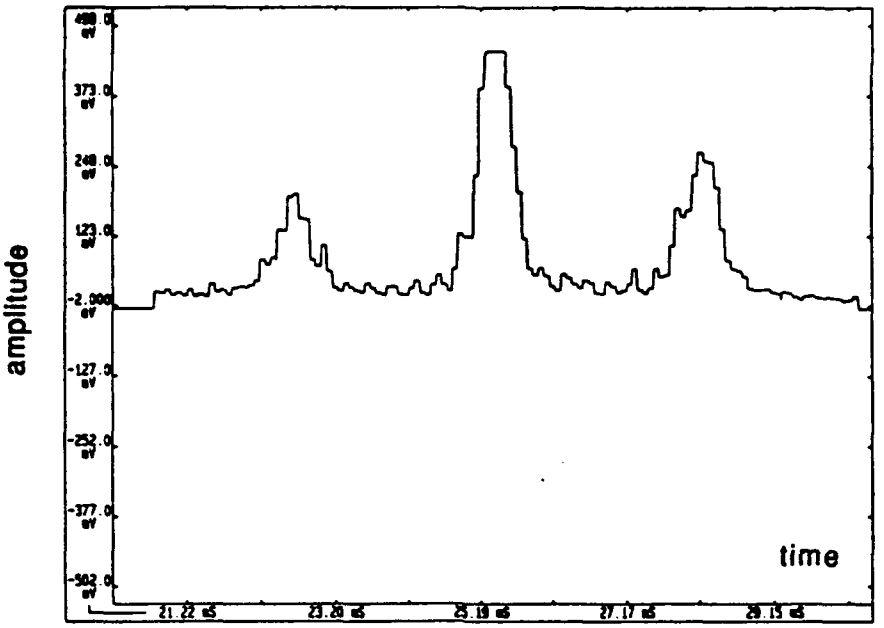

(a) Unfiltered signal

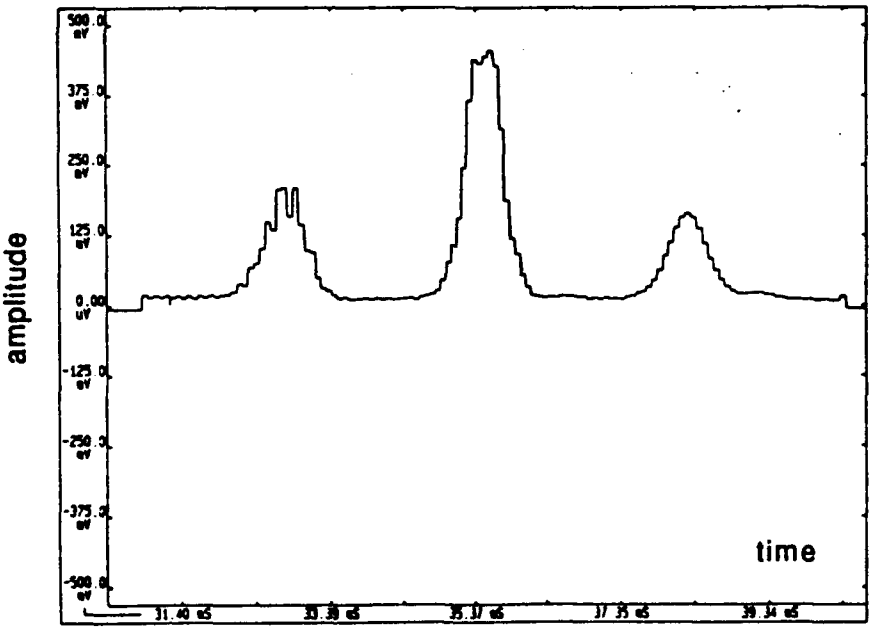

(b) With spatial filter, pinhole size = 0.00292 inch

Figure 2.3.3 Digital oscilloscope trace of filtered vs. unfiltered optical signal

2.3.3 Oscillations from the LCTV

Testing of the LCTV as a spatial light modulator revealed another undesirable property, namely, a 60 Hz oscillation of the optical signal (figure 2.3.4). This was not observed in early tests due to the averaging effects of the detector used. However, subsequent tests with a fast detector revealed this problem. Room lights, AC power, and the laser itself were eliminated as possible sources of this oscillation. The LCTV was operated with room lights off, and from a DC power source, and the problem remained. There was no oscillation when the laser alone illuminated the detector.

The problem is apparently due to the video refresh rate of the TV screen (alternate lines refreshed at 30 Hz, giving an overall apparent oscillation of 60 Hz). Correction of this problem will require a modification of the drive electronics of the LCTV, possibly to an active matrix drive system which addresses each pixel individually, or the use of a different SLM in the system.

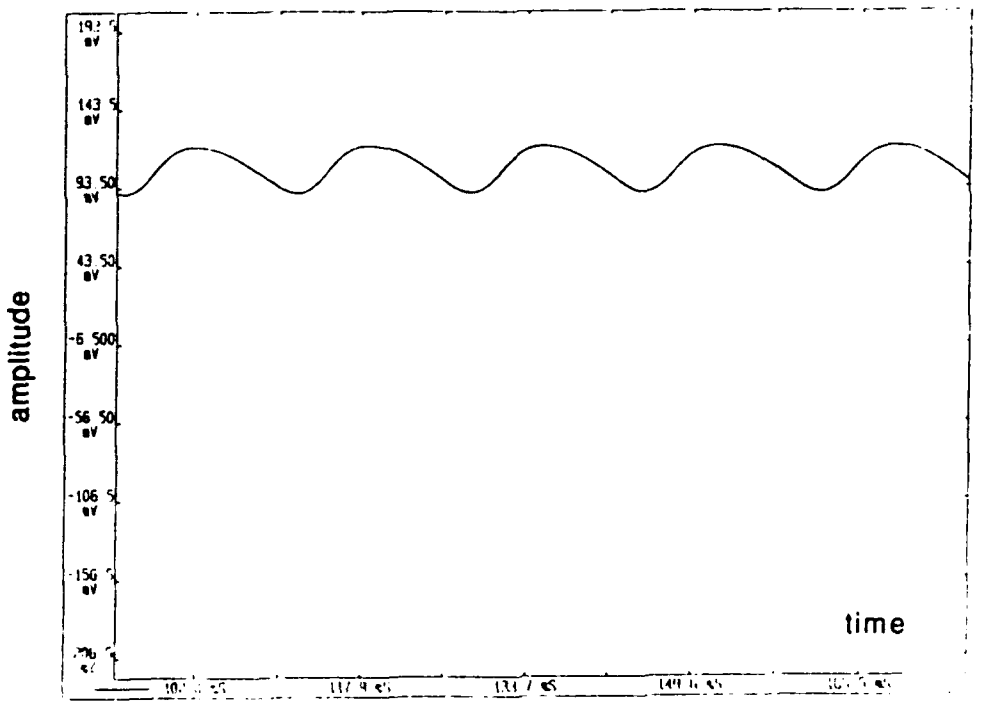

Figure 2.3.4 60 Hz oscillation observed on LCTV

2.4 Alternative spatial light modulators

The LCTV was initially chosen as a low cost means of validating certain concepts in this proof-of-principle hybrid architecture. It has certain properties, such as size, ease of use,

and pixel structure, in addition to its attractive low cost, that make it well suited to preliminary laboratory investigations in this area. However, the 60 Hz oscillation problem, however, must be eliminated if the device is to be used in our proposed signal processing application.

It may not be possible to adequately modify the driving electronics, since the problem is really with the liquid crystal pixels themselves. This type of liquid crystal (twisted nematic) requires a constant voltage at each pixel, in order to keep each pixel switched on. There are other types of SLM's which do not require constant voltage inputs at each pixel, and thus should be free of the oscillation problem.

The Semetex Sight Mod magneto optic SLM is an example of a SLM which does not require constant voltage inputs at each pixel. We were able to temporarily acquire a Sight Mod for testing purposes, and so we performed the same weight pattern test considered above. The particular device we used had an active area consisting of 128X128 pixels, with pixels 56 μm on a side.

Figure 2.4.1 shows the results of this test. The ratio of the height of the center peak to the side peaks here is approximately 5:1, rather than the expected 3:1. It is conjectured that this may be due to the diffraction effects caused by the small pixel size. Further testing will be needed to isolate the exact cause of this problem and investigate possible remedies. If this effect can be consistently predicted, it may be possible to correct for it when writing the weight patterns to the screen. Extremely low optical transmission (approximately 6% has been reported) is another undesirable property of this SLM.

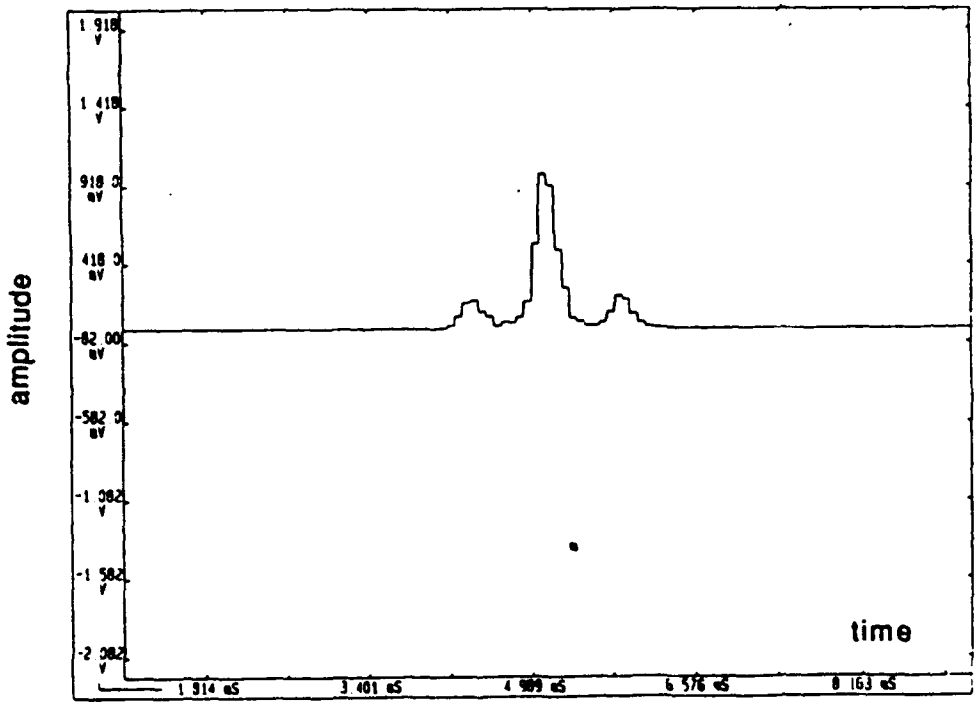

Figure 2.4.1 Results from the Semetex Sight Mod

On the positive side, the 60 Hz oscillation problem was not present when using this SLM.

Another possibility to consider for spatial light modulation is a ferroelectric liquid crystal display, such as those distributed by Displaytech, Inc. These are smectic (as opposed to nematic) liquid crystals, and they exhibit bistability. That is, when they are switched "on", they stay "on" indefinitely (at least, up to a couple of hours) without applied voltage. Although we have not tested such a device, its properties appear to make it a promising candidate for our SLM needs. Displaytech has available a 128X128 device, with pixel size approximately 150 μm, 16 μm spacing between pixels, and frame speed of 100 Hz.

For future reference, we list here the properties we desire from a SLM for this application. Although there does not exist at the present time a device satisfying everything on this list, it will be good to keep this list in mind when selecting SLM's for this application.

Desired SLM properties:

1. The pixel array size should be at least 100X100. In one dimension, we need at least 100 weight vector components, otherwise there is no point in doing this processing optically. In the other dimension, we need 100 elements to achieve 100:1 dynamic range in the numerical representation of the components.
2. We require only binary operation at the pixel level (ie., "on" and "off"). However, we do need high contrast ratio, that is, we need "off" pixels to block nearly 100% of the incident light, and we need "on" pixels to transmit as much light as possible. Of these two, it is more important that "off" pixels be really "off", as we can compensate somewhat for low optical transmission through the "on" pixels by using more laser power.
3. Bistable operation at the pixel level, ie., pixels that are switched "on" stay "on" without additional voltage being applied (this will eliminate any oscillation problems) would be desirable.
4. We can use as much frame speed as can be delivered. The output from our SLM configuration will interact with an acousto-optic cell, so we can handle just about any output speed. The device should be capable of at least video rates (30 Hz), and preferably should have frame speeds on the order of 100 Hz or more. .
5. Active area display size should be compatible with normal optics, ie., on the order of a few cm per side. Pixel size should not be so small as to cause diffraction problems. Spacing between pixels should not be so large as to cause excessive light leakage problems.
6. Device should be able to be driven by a microprocessor, so that we can write weight patterns upon it.
7. Transmissive operation mode is preferred, although the system design could be modified to accomodate a reflective device.

2.5 Patent application

We have applied for an Air Force patent for our use of a two dimensional SLM display as an extended dynamic range one dimensional SLM. Such devices could be used anywhere

that optical representation of one dimensional numerical data is desired, such as signal processing applications, phased array antenna steering, and neural network architectures. The device is intended to operate as shown in figure 2.3.1. A diagram of the device as it appears in the patent application is shown in figure 2.5.1.

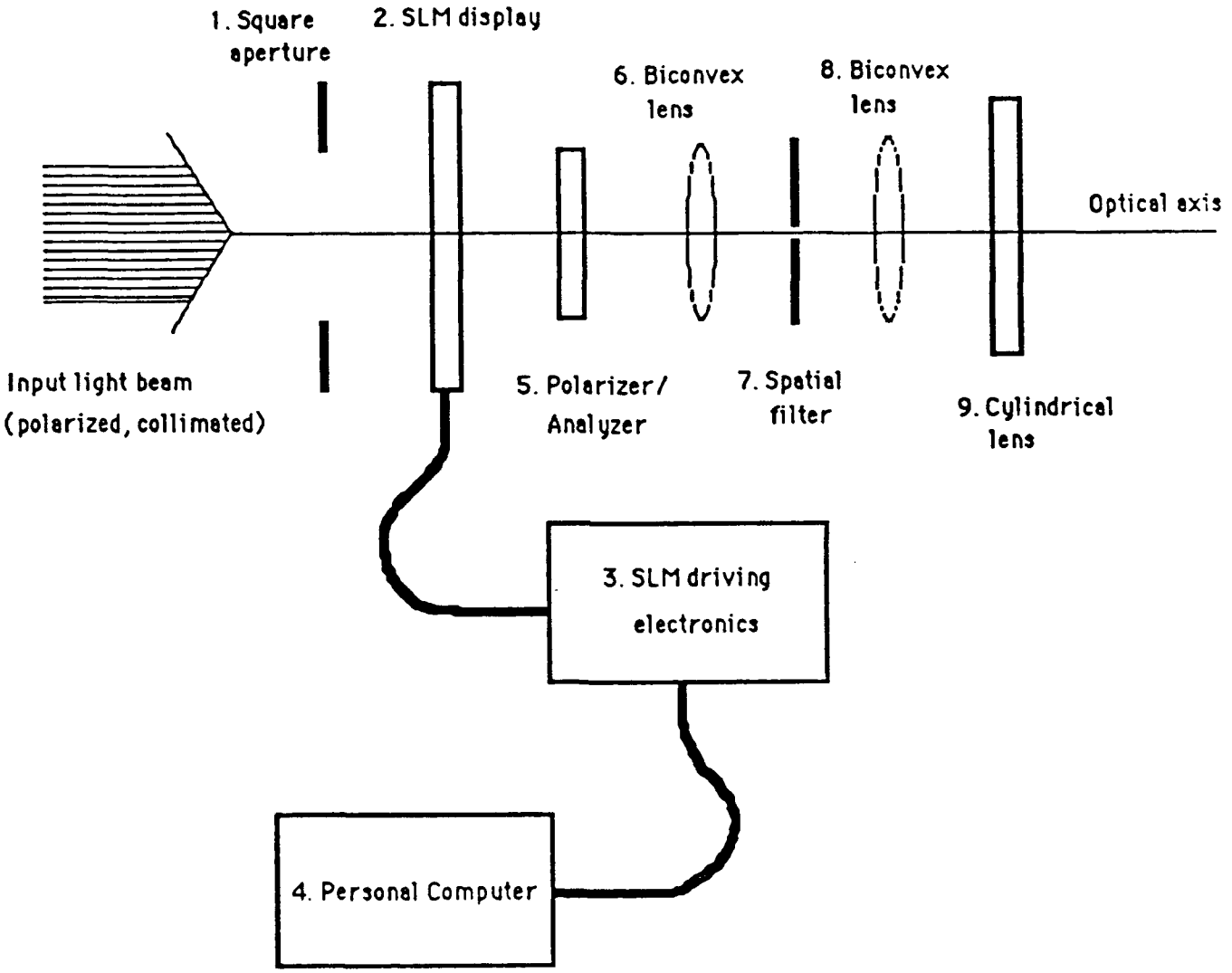

Figure 2.5.1 Extended dynamic range 1-D spatial light modulator (top view), patent applied for

3. SYSTEM TEST PROCEDURES AND TEST RESULTS

As shown in the block diagram of figure 2.2.1, the processor can be thought of as consisting of two optical subsystems connected by a personal computer (PC). This configuration is advantageous for testing purposes, since each optical subsystem can be tested separately before the entire system is tested. The two optical subsystems are independent of each other, and the order in which they are tested does not matter. We discuss test procedures for the second subsystem first, since it is the easier of the two to test. We have in fact begun its testing, and we report those results here also.

3.1 Test procedures for the second optical subsystem

Details of the test setup for the second optical subsystem, including appropriate supplementary electronics, are shown in figure 3.1.1. The purpose of the second optical subsystem is to take the weight vector computed by the first optical subsystem and the PC and recombine it with the auxiliary signal $n_1(t)$ to produce an estimate y(t) of the noise/jamming signal n(t). Thus, the second optical subsystem can easily be tested by setting up a signal scenario in which the correct weight vector is known, and providing this weight vector as input. If the system is working correctly, it should produce a signal y(t) which closely estimates the interference n(t), so that the difference n(t) - y(t) can be observed on an oscilloscope as being close to zero. That is, if we give the system the right answer, we can see if it knows what to do with it.

For the purpose of testing this subsystem, and indeed, for testing the entire processor, we should keep in mind the following simple example problem that we are trying to solve: given a signal $n_1(t)$, and another signal n(t) of the form $A*n_1(t - \delta)$ for some fixed positive numbers A and δ, determine A and δ. This is the essence of the noise/jammer cancellation problem. If we can't solve this problem, then we can't solve more complicated problems involving multiple copies of $n_1(t)$ with different A's and δ's, the presence of a main signal, etc., so there's no point in worrying about them.

In the context of this simple problem, the second optical subsystem takes a given A and δ and attempts to form the signal $n(t) = A*n_1(t - \delta)$. We denote by y(t) this output of the optical system which is an estimate of n(t). We test how close y(t) is to n(t) by subtracting them electronically and observing the result on an oscilloscope.

3.1.1 Introducing A and δ into the optical system

The value of δ should be restricted to be between 0 and the total aperture delay time of the acousto-optic deflector modulator (ADM), in our case 5 μsec. Suppose a value of 2 μsec is chosen, with a total ADM aperture time of 5 μsec. This single delay value will be represented on the SLM as a single vertical bar of "on" (transmissive) pixels, located 2/5 of

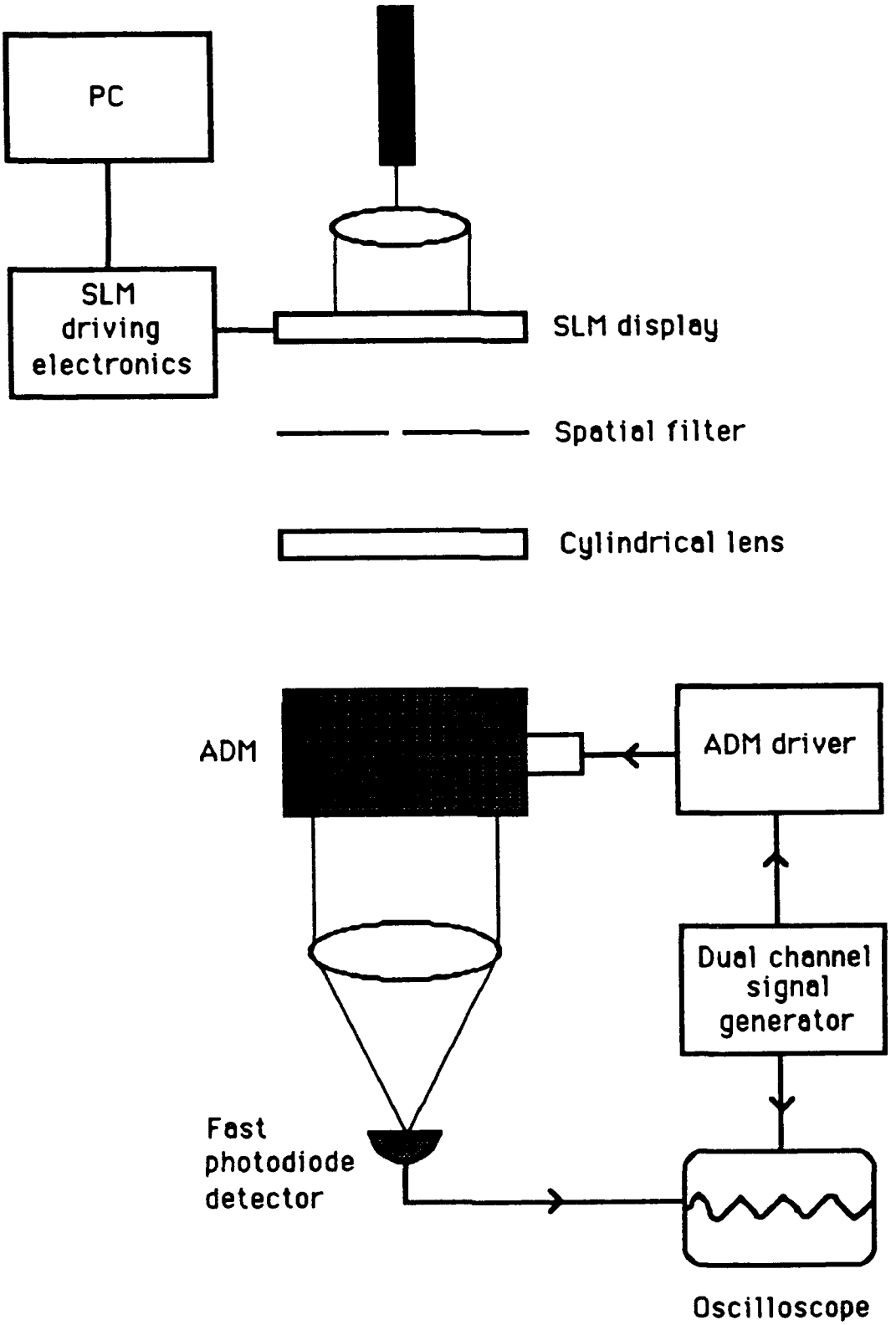

Figure 3.1.1 Test setup for the second optical subsystem

the way across the screen (2 μsec/5 μsec). From which side? We want the light coming through the SLM to "pick out" the auxiliary signal when it is 2/5 of the way through the ADM. That is, the light should illuminate a spot on the ADM a distance 2/5 of the total aperture distance from the *transducer end* of the ADM. So, the vertical bar on the SLM should be 2/5 of the way across the active area of the SLM display, measured from the side of the display closest to the transducer end of the ADM (see figure 3.1.2).

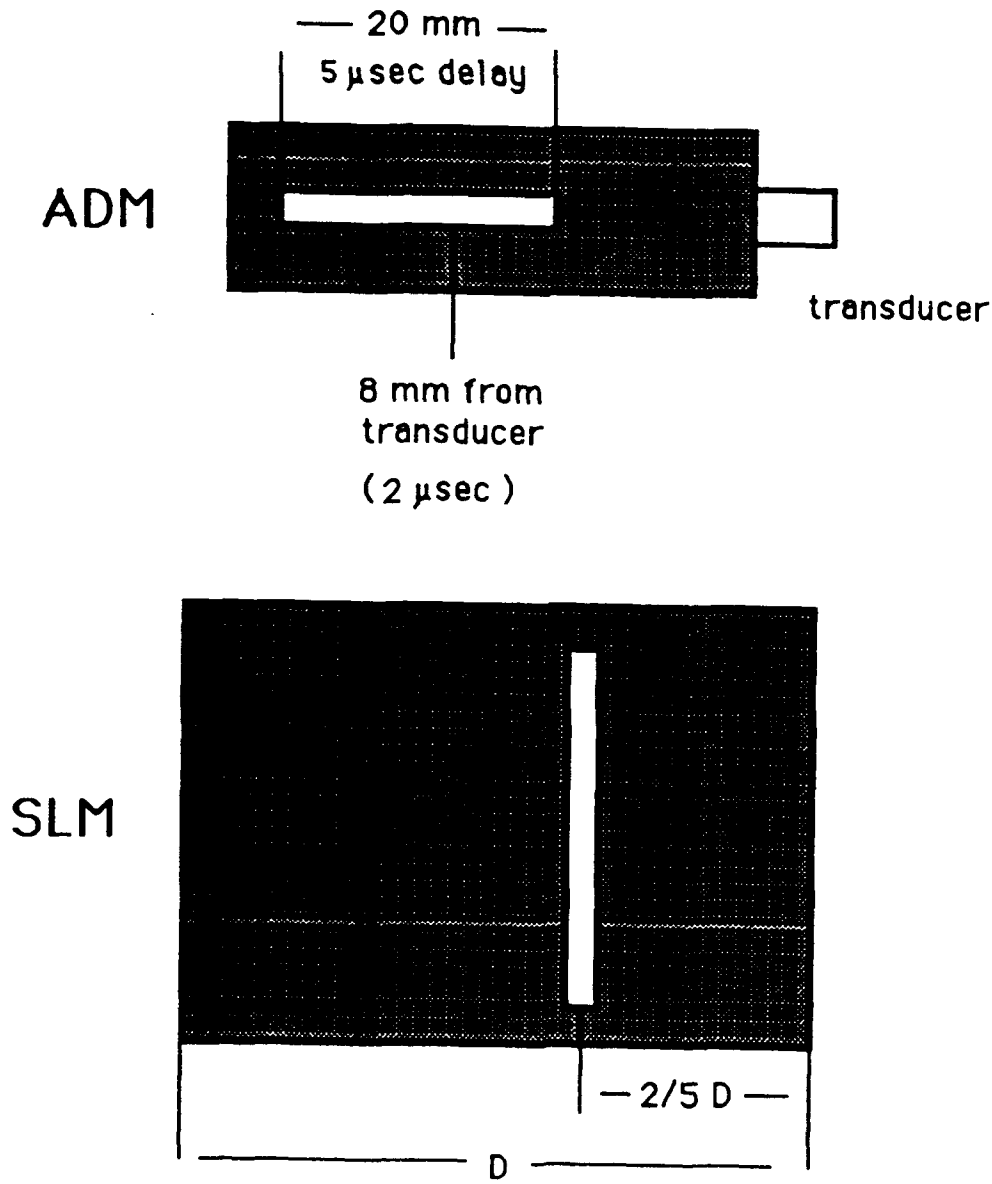

Figure 3.1.2 Positioning of SLM pattern relative to ADM

The ADM should be positioned at the correct Bragg angle ϕ. This angle is given by

$$\sin \phi = \alpha/2\beta$$

where α is the optical wavelength, and β is the acoustic wavelength in the crystal medium. With a HeNe laser at 633 nm, and a 40 MHz carrier signal in the flint glass crystal (acoustic velocity 20 mm/5 μsec), this works out to sin ϕ = 0.003165, or ϕ = 0.003 radians (0 degrees, 10 min, a small angle!). In practice, correct positioning of the ADM is achieved by positioning it on a rotating mount, and then rotating the ADM until good separation between the 0 and 1rst orders is obtained.

On output from the ADM, we want only the first order light; the 0 order should be blocked. One possible optical configuration to achieve this is shown in figure 3.1.3 (the Bragg angle in this picture is obviously exaggerated for clarity here).

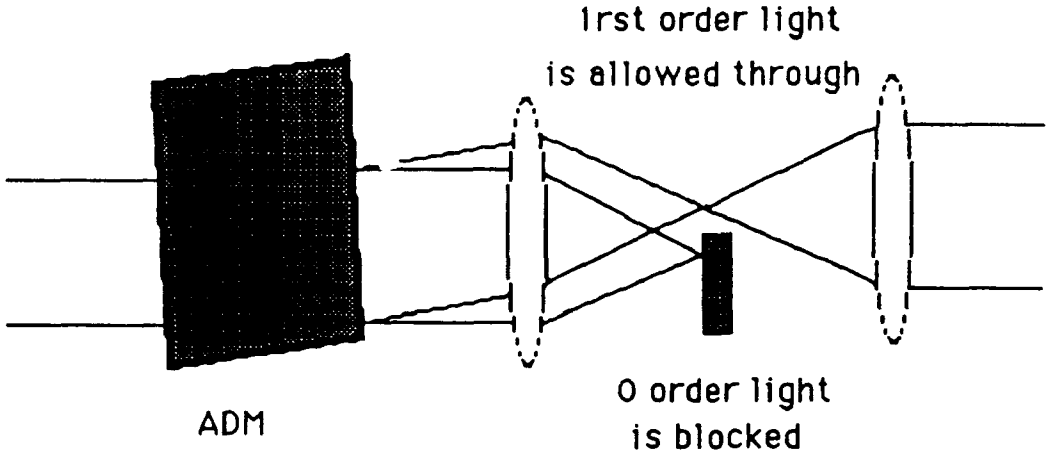

Figure 3.1.3 Optical configuration to block 0 order output from ADM

The amplitude of the optically produced output signal can be adjusted by varying the height of the vertical bar on the SLM display. Optical amplitude will also be affected by transmission losses throughout the optical system. The amplitude of the electronically produced signal can also be adjusted at the signal generator so that a match between the two amplitudes can be achieved.

3.1.2 The signal electronics

For testing purposes, we need a signal generator capable of generating a signal $n_1(t)$ together with a delayed version $n(t) = A*n_1(t - \delta)$, where δ is at least a few μsec. In practice, this delay will most likely be produced by varying the phase of a second output signal. For testing purposes, signal frequency is not significant. It can be a few kHz. However, the final system should be able to accomodate frequencies up to 5 MHz.

We also need summing electronics capable of subtracting one signal from another. This

can be accomplished most easily with an oscilloscope, which can also be used to observe the final output.

The test will be successful if we can observe essentially a zero signal on the oscilloscope when the optics system is active and n(t) is input from the electronics. When the optics system is interrupted, we should observe just the signal n(t) on the oscilloscope.

The signal $n_1(t)$ represents the auxiliary signal (the signal coming from the omni-antenna), while n(t) represents the noise or jamming signal. Thus, $n_1(t)$ is used as input to the ADM, while n(t) goes to the summing electronics.

3.1.3 Test results for the second optical subsystem

We were able to setup a test of the second optical subsystem. The test configuration was similar to that shown in figure 3.1.1. Since the LCTV exhibited the 60 Hz oscillation problem discussed earlier, we substituted a fixed mask consisting of an index card with a vertical bar cut into it as an ideal "spatial light modulator". This card was mounted on a translation stage so that the relative position of the vertical bar could be changed.

The appropriate signals were generated using a Hewlitt Packard Model 3326A Two Channel Synthesizer. This device can produce two signals with a relative phase difference and adjustable amplitudes. One signal was sent directly to a digital oscilloscope, while the other was input to the ADM driver (where it modulated a 40 MHz carrier). We used 1 MHz sinusoidal signals for this test.

The output of the optical system was collected with a photodiode detector, and the resulting signal was sent to the digital oscilloscope, where it was subtracted from the electronically generated signal. By moving our "SLM" on the translation stage, we were able to achieve signal cancellation. The results from the digital oscilloscope are shown in figure 3.1.4.

The amplitude of the optical signal was fairly small due to low initial laser power and optical transmission loss. The electronic signal amplitude was lowered correspondingly so that signal cancellation could be achieved. The result of these low amplitudes was that digitization noise became fairly dominant in the plots shown in figure 3.1.4. It is difficult to judge the true cancellation performance from this noisy data. We hope to repeat this test with a more powerful laser, and, hence, larger amplitude signals.

What this test showed is that using an acousto-optic cell and a spatial light modulator we can optically produce a signal that matches an electronically produced signal. In some sense, this test shows us the best cancellation that we can hope to achieve, since our fixed mask "SLM" was ideal, in the sense of perfect contrast ratio and perfect positional freedom via the translation stage. No amount of algorithm development or money spent on exotic SLM's can improve upon this performance (with this particular laser/optics/ADM setup).

The second optical subsystem can thus be tested in this way, independent of the SLM, to determine a benchmark performance that can then be used to evaluate the performance of actual SLM devices inserted into the system.

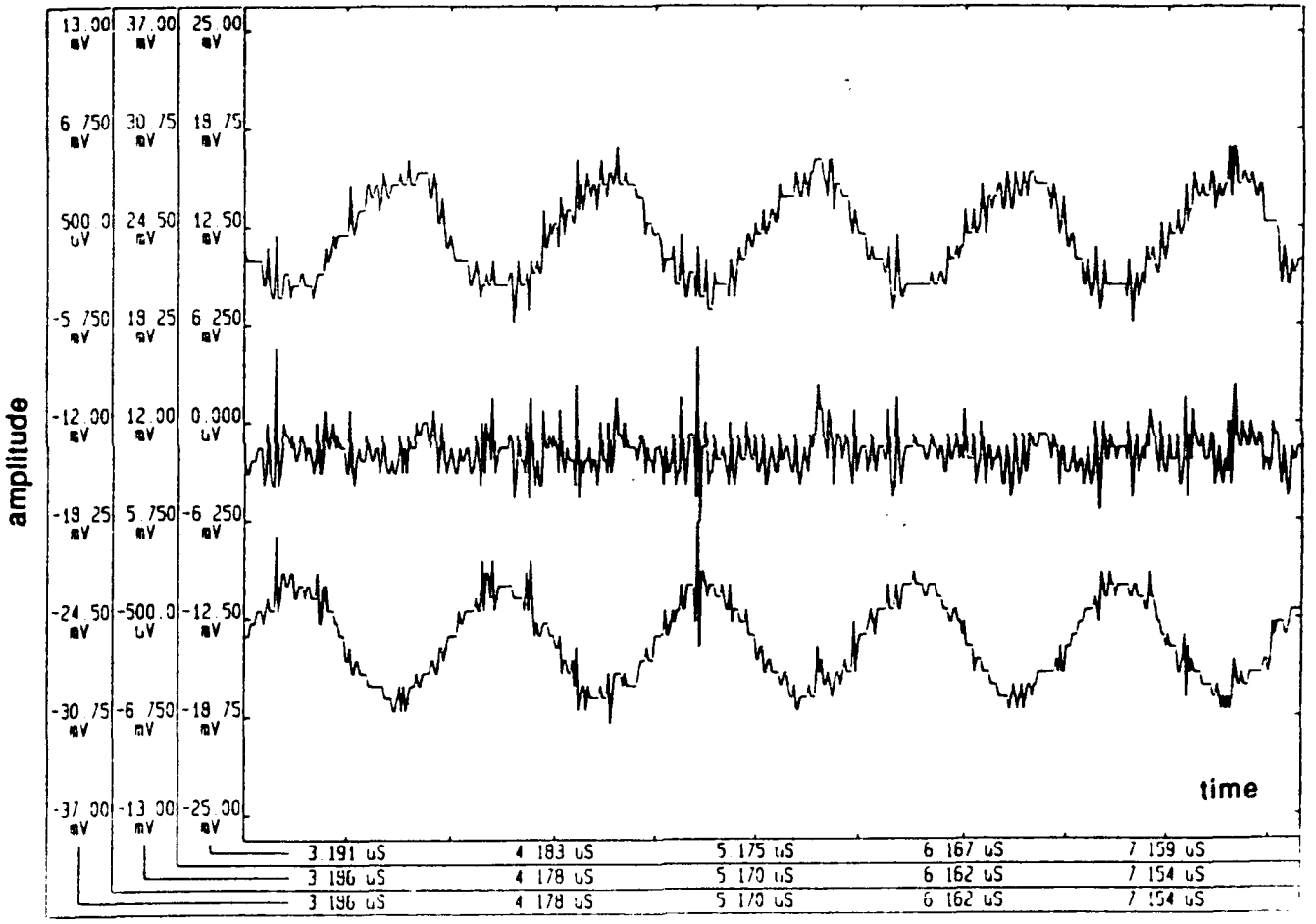

Figure 3.1.4 Digital oscilloscope plot of cancellation test (the upper signal is the optically generated signal, the bottom signal is the electronically produced signal, with the cancellation signal in the middle)

3.1.4 Additional testing of the second optical subsystem

It would be desirable to test the second optical subsystem with the alternative SLM's mentioned above in paragraph 2.4, namely, the Semetex Sight Mod and the Displaytech ferroelectric liquid crystal device. The complete processor cannot be tested until a suitable SLM is found that can be modulated in real time (30-100 Hz), and that is not subject to the oscillation problems of the LCTV.

As an optional advance test, it would be desirable to be able to generate a noise signal of the form $n(t) = A_1 n_1(t - \delta_1) + A_2 n_1(t - \delta_2)$. That is, generate two different delays of the same signal $n_1(t)$. This would simulate "multipath" effects (multiple reflected copies of the same jamming signal).

It will be relatively easy to set up the optical system to accomodate this test. We simply put two vertical bars on the SLM display to correspond to the two delays (although it may take some trial and error to match the relative positions of the bars to the delays). The difficulty at the present time is in obtaining the appropriate electronics to generate two different delayed versions of the same reference signal. We need either a signal generator with three outputs (reference and two delayed or different phased versions) or some type of external delay device. It may also be possible to use the digital oscilloscope to play back recorded waveforms as a means of producing signals.

Since the ability to handle "multipath" is one of the anticipated benefits of such an optical signal processor, this would be a desirable test to perform.

3.2 Testing the first optical subsystem

The purpose of the first optical subsystem is to form the weight update vector. The weight update vector is added to the old weight vector stored in the PC to produce the new weight vector. If our optical output signal y(t) is far off from the signal n(t) it is trying to estimate (so that y(t) - n(t) has a large amplitude), then the weight update vector will have large components. Similarly, if y(t) - n(t) is small, then the weight update vector will be small as well.

Unfortunately, y(t) comes from the second optical subsystem, so that in testing the first subsystem by itself we will not have y(t) available. All we can do to test this part of the system is to produce an artificial signal input and ensure that a reasonable weight update vector is being produced for this input.

3.2.1 The test setup

Details of a test setup for the first optical subsystem are shown in figure 3.2.1. Once again, we will need to produce a signal $n_1(t)$ and a delayed attenuated version

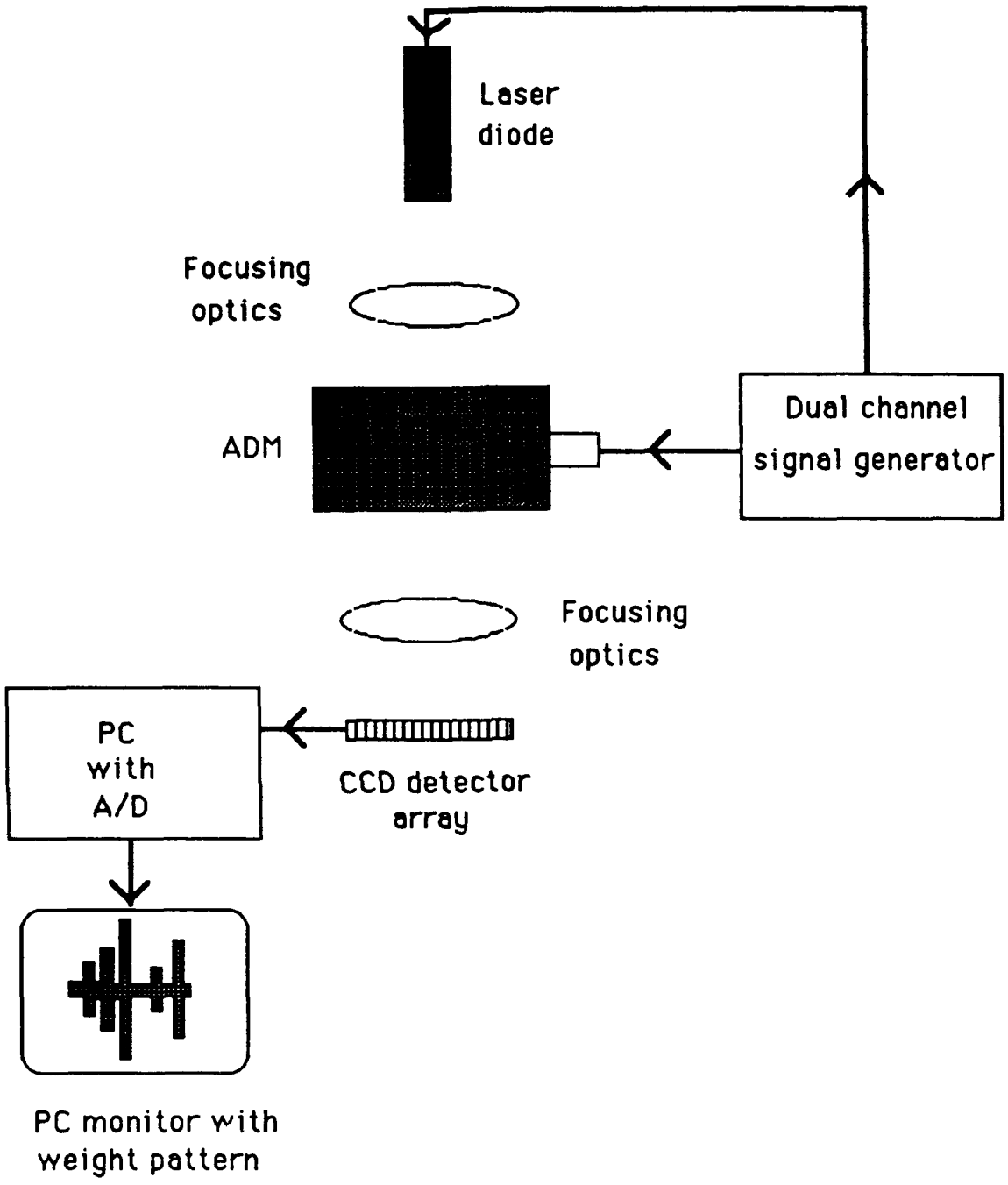

Figure 3.2.1 Test setup for the first optical subsystem

$n(t) = A*n_1(t - \delta)$, although here the delay is not critical. The $n_1(t)$ signal is used to drive the ADM (after being placed on a 40 MHz carrier). The signal n(t) drives a laser diode. It would be useful to be able to apply a variable attenuation on n(t) and observe the resulting vector that the system produces. As the amplitude of n(t) decreases we should be able to observe a decrease in the components of this vector.

Here, as in the second optical subsystem, the ADM should be aligned at the Bragg angle, and we want only first order light output. The zero order light should be blocked as shown in figure 3.1.3.

The optical output of the ADM is collected onto a CCD array. Integration time for the CCD array should be on the order of 10 msec. The output from the CCD array goes to the analog-to-digital (A/D) converter, which is part of the PC. A pattern representing the system output vector can be written on the PC monitor screen.

As an example of a "reasonableness test", it should be possible to visually compare the pattern on the computer screen with the actual light pattern incident on the detector array. The computer pattern will be very much like a histogram, and the longer vertical bars in this pattern should correspond to the brighter spots of light on the detector array.

3.2.2 Data acquisition and timing

The A/D converter is actually a board located in the PC. Special software is required in order that the PC can communicate with this board and data acquisition can occur. A significant part of this first optical subsystem test will be to verify that optical information impinging on the CCD array is correctly being communicated to the PC. Among the issues to be resolved are the timing of the CCD array, timing of the A/D board, and how fast the PC can accept data and still write weight patterns on the screen.

As a starting point, we should consider using an integration time of 10 msec on the CCD array. Thus, 100 times per second, the CCD array will provide an analog signal as input to the A/D board. We would like something on the order of 100 weight components, so we should probably sample the analog input at 300 points and average. This places a data requirement of 30,000 samples per second on the A/D board, which should be well within its capabilities.

A more critical concern is whether the PC can deal with this data rate. In the final system, the PC must be able to accept 300 sample points, average them to produce a weight update vector with 100 components, add the weight update vector to the old weight vector to produce the new weight vector (possibly computing a variable stepsize as well), and write the new weight vector pattern to the screen, all in 10 msec. Should the PC not be able to keep up with the data rate, it may be necessary to average several weight update vectors before producing a screen output. We can also lengthen the integration time on the CCD array, although this will degrade the overall performance of the complete system.

The A/D converter may produce extraneous sample values due to high frequency noise. If this is the case, it may be necessary to send the analog CCD output through a low pass filter prior to A/D conversion.

3.3 Testing the complete processor

Setting up a test of the complete processor should be relatively straightforward, once the above tests of the two optical subsystems have been completed. We should start with the simple example used to test the second subsystem, involving $n_1(t)$ and a noise/jammer signal n(t) of the form $A*n_1(t - \delta)$. The same $n_1(t)$ signal drives each ADM. The signal used to drive the laser diode in the first subsystem is now y(t) - n(t), where y(t) is the optical output of the second subsystem.

The signal y(t) - n(t) should be displayed on an oscilloscope. When the processor is working correctly, this signal should eventually become 0. System performance is determined by comparing the amplitude of this difference with the amplitude of n(t).

The following paragraphs describe some things to keep in mind when testing the complete processor.

3.3.1 Feedback

The complete processor operates as a feedback loop. There are advantages and disadvantages associated with this.

The good news is that the feedback serves to adaptively control errors. This a virtual necessity for any type of analog processor, since such processors will naturally tend to drift away from the correct answer when operating over a period of type, unless some type of control is imposed on them. This feedback control in our processor may be able to compensate for some optical aberrations and other undesirable component properties. We hope, however, that system inaccuracies don't eat up all of the adaptive capacity of the processor.

The disadvantage associated with feedback is that it introduces the potential for stability problems. Fortunately, our modular design consisting of two independent subsystems means that we need only be concerned with stability from an algorithmic point of view. Since there is no optical feedback, we do not need to worry about chaotic laser pumping, for example.

The PC acts as an "escape valve" to control feedback. The scalar stepsize parameter, used as a multiplier of the weight update vector, is critical for controlling algorithmic stability. A way of dynamically varying this parameter is described in section 4.3. There will likely be other software enhancements necessary to achieve optimal stable performance.

3.3.2 Processing data in the PC

The A/D data for the weight update vector should be scaled to be between -1 and 1. This allows the weight vector to be adjusted in either the positive or negative direction. Negative

update values are a necessity, otherwise we would have no way of reducing weight vector component values in order to change the weight vector itself.

The weight vector itself is not allowed to have negative values, but rather its component values are restricted to be between 0 and 1. Negative weighting, if needed, can be accomplished by assigning positive values to those components corresponding to 180 degree phase shifts.

If necessary, vector "masks" can be applied to either the weight update vector or the weight vector itself to compensate for nonlinear optical effects. For example, if the weight pattern on the SLM is to be illuminated with a Gaussian beam, then an inverse Gaussian mask can be digitally applied to the weight vector prior to output from the PC, cancelling Gaussian effects in the resulting spatial light pattern. It may also be possible to compensate for some of the nonlinear effects of the ADM's in this way. The system adaptivity may take care of some of these effects, but if they can be anticipated, and they are hardware rather than signal dependent, then the convergence speed of the processor should be improved.

3.3.3 The weight vector solution

In setting up test involving a noise signal n(t) which corresponds to a single delayed version of the auxiliary signal $n_1(t)$ (that is, $n(t) = n_1(t - \delta)$ for some fixed δ), one would expect to see a weight pattern consisting of a single vertical bar. However, it may be that there is more than one appropriate weight vector solution, particularly if we deal with high frequency signals. For example, if a 1 MHz signal is delayed 1 μsec, we get the same signal back again. In a 5 μsec delay aperture, there are 5 copies of such a signal. Any of these copies, or any linear combination of these 5 copies, could be used to cancel the original signal. The resulting weight pattern could, for example, consist of 5 equi-spaced small vertical bars, rather than one large vertical bar.

Thus, you may not see the weight pattern on the SLM that you are expecting to see. This is all right as long as the signal output n(t) - y(t) converges to 0.

4. SYSTEM CONSIDERATIONS

In this section we consider various aspects of this electro-optic design that will affect overall system performance. The purpose of the following sections is to anticipate certain problem areas, so that when the processor does not perform as expected, these areas can be investigated as possible sources of inaccuracies. In particular, we look at the possible effects of limited dynamic range, and the effects of light leakage through the SLM. On a positive note, we also look at a way which the microprocessor can be used to improve system performance by dynamically varying the algorithm stepsize.

4.1 The effects of limited dynamic range

In an analog system that attempts to do numeric processing, dynamic range can be thought of as a limit on the number of resolvable numeric values that can be achieved by the system. The two optical subsystems of our processor are analog systems and so are subject to the effects of limited dynamic range.

To study the effects of this limited numerical resolution, a computer simulation was carried out. The algorithm of section 2.1 was used with simulated signal input. Limited numeric accuracy was imposed on the system in two places: at the input to the algorithm and at its output. These correspond to the two optical subsystems. The input comes from the CCD array and the A/D converter, and the output is what the SLM/cylindrical lens combination presents to the second acousto-optic cell. A block diagram is shown in figure 4.1.1.

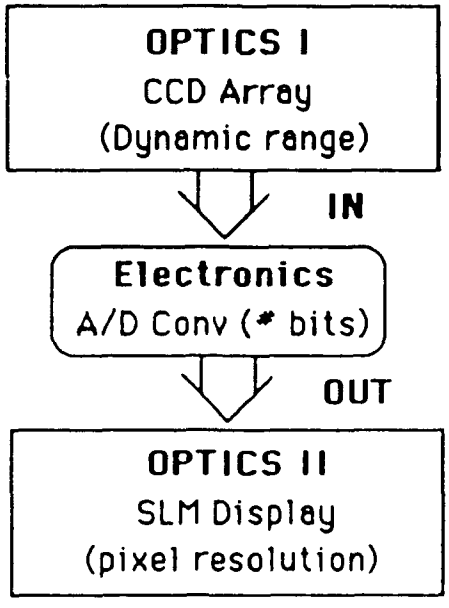

Figure 4.1.1 Where limited numeric resolution enters the system

The computer simulation was set up so that the number of numeric values could be independently adjusted for input and output. Figure 4.1.2 (a) shows the graphic output of the simulation with unlimited accuracy (up to the 16 bit accuracy of the PC) available on both input and output. The graph shows the remaining noise after cancellation. The amount of cancellation is over 50 dB (the starting noise/jammer amplitude is 1.0). This is what the algorithm can deliver with unlimited accuracy.

Figure 4.1.2 (b) shows the results when the number of output resolvable values is reduced to 50 (such as would happen with a SLM with only 50 pixels in the vertical direction). The performance drops to 15 dB. With 100 values available (ie., 100 vertical pixels) this improves to 22 dB (figure 4..1.2 (c)). Both of these examples were run with no limit on input accuracy.

Next, the input accuracy was limited to 256 resolvable values (such as would occur with an 8 bit A/d converter, or a CCD array with a dynamic range of 256:1), with the output kept at 100. The performance remained at 22 dB, as shown in figure 4.1.2 (d). The good news here is that the effects of limited dynamic are not additive. That is, the system performance seems to be affected only by the component with the worst numerical accuracy, and is not cumulatively affected by each occurrence of limited accuracy that is encountered.

This simulation shows, however, that we cannot expect to attain the desired system performance of 40 dB cancellation as long as there is a component that is limited to 100 levels of numerical accuracy. To achieve 40 dB, a numerical resolution of about 1000 is needed on input and output. Figure 4.1.2 (e) shows the results of using this level of accuracy on input and output, with a performance of 43 dB in this case. We can easily obtain 1000 levels on input, since CCD arrays routinely claim a dynamic range of more than 1000:1 (some claim 1,000,000:1), and 10 or 12 bit A/D converters exist that run at a fast enough speed for our purposes. However, on output we do not currently have available an SLM that will deliver the required accuracy. This would require 1000 pixels in the vertical direction with our current configuration. Alternatively, it may be possible to achieve increased accuracy from an SLM that has several resolvable levels at each pixel, rather than just a binary operation.

In Section 4.3 we discuss a modification to the algorithm in the PC that improves the system performance in the case of 100 output levels to 29 dB.

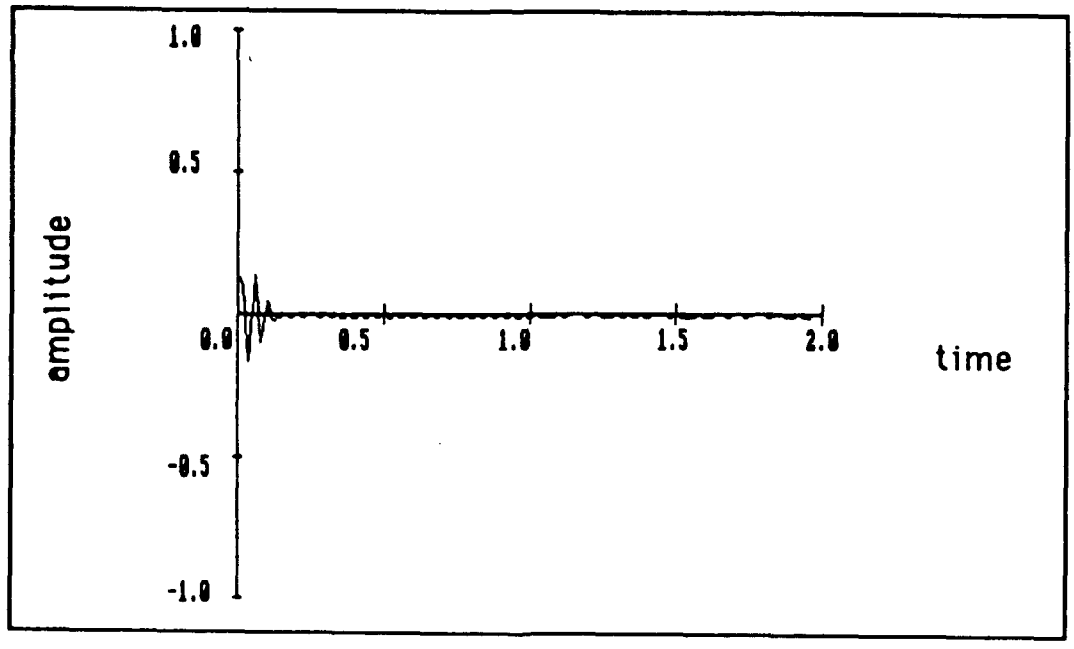

a) unlimited resolution in and out

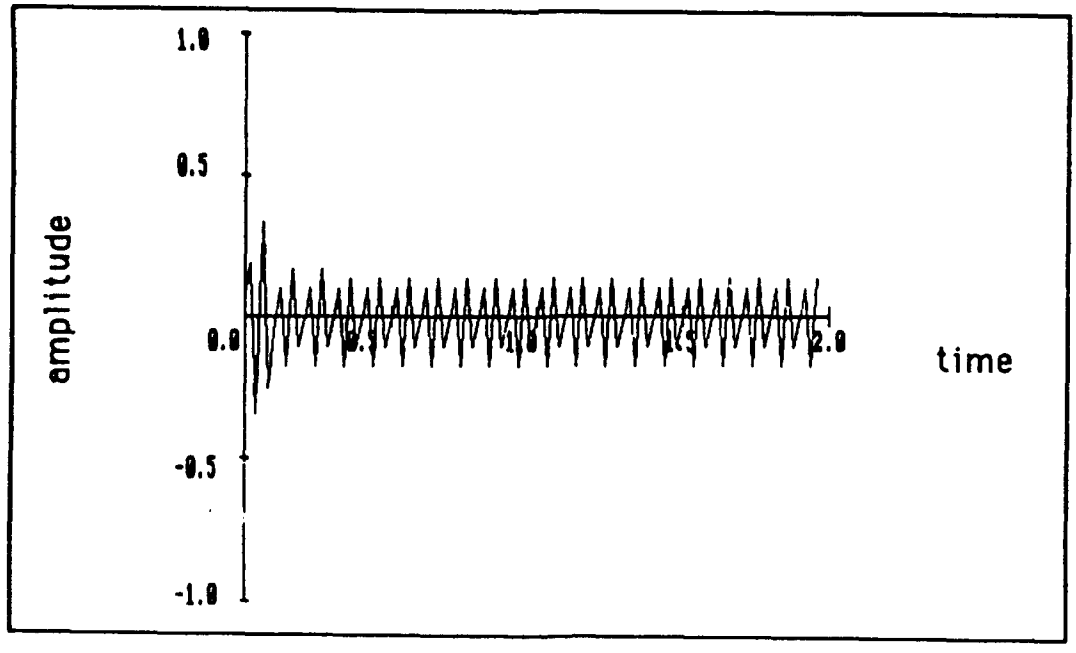

b) unlimited in, 50 levels out

Figure 4.1.2 The effect of limited numerical resolution

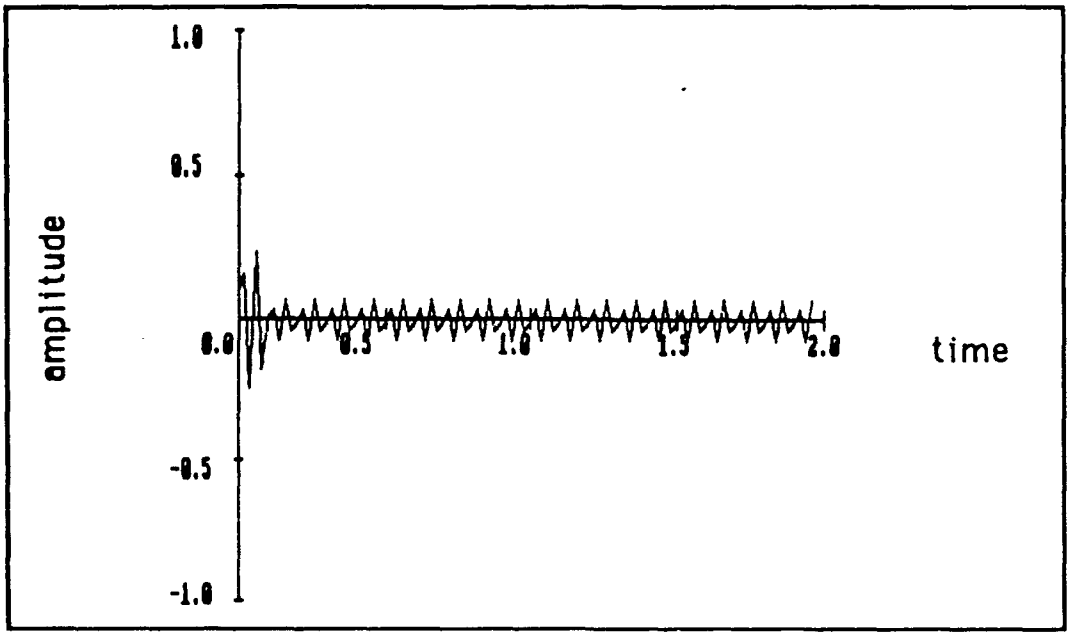

c) unlimited in, 100 levels out

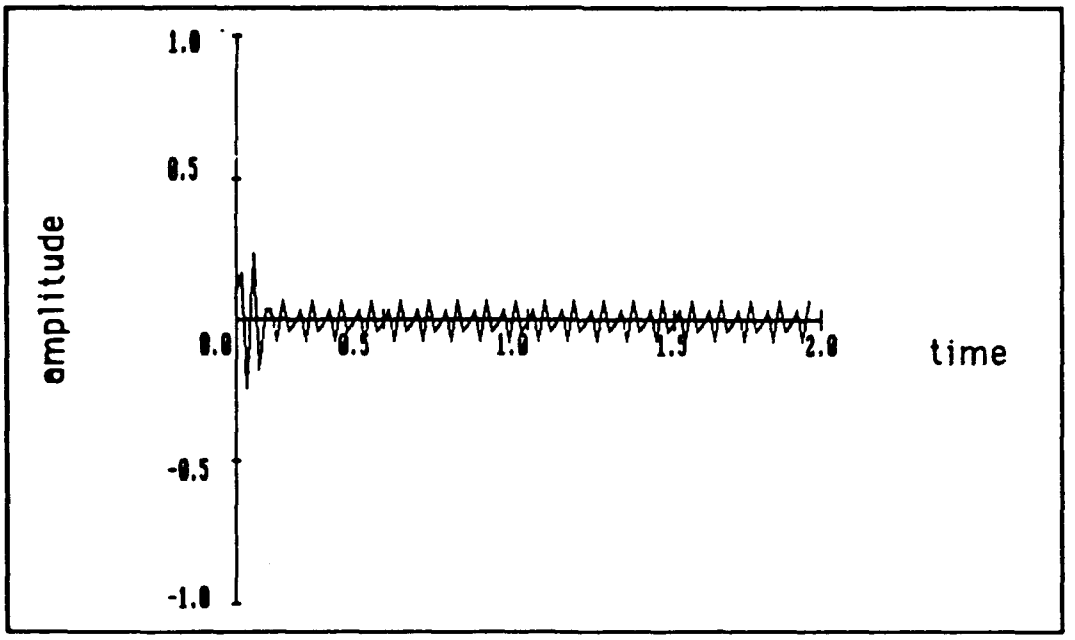

d) 256 levels in, 100 levels out

Figure 4.1.2 (cont'd) The effect of limited numerical resolution

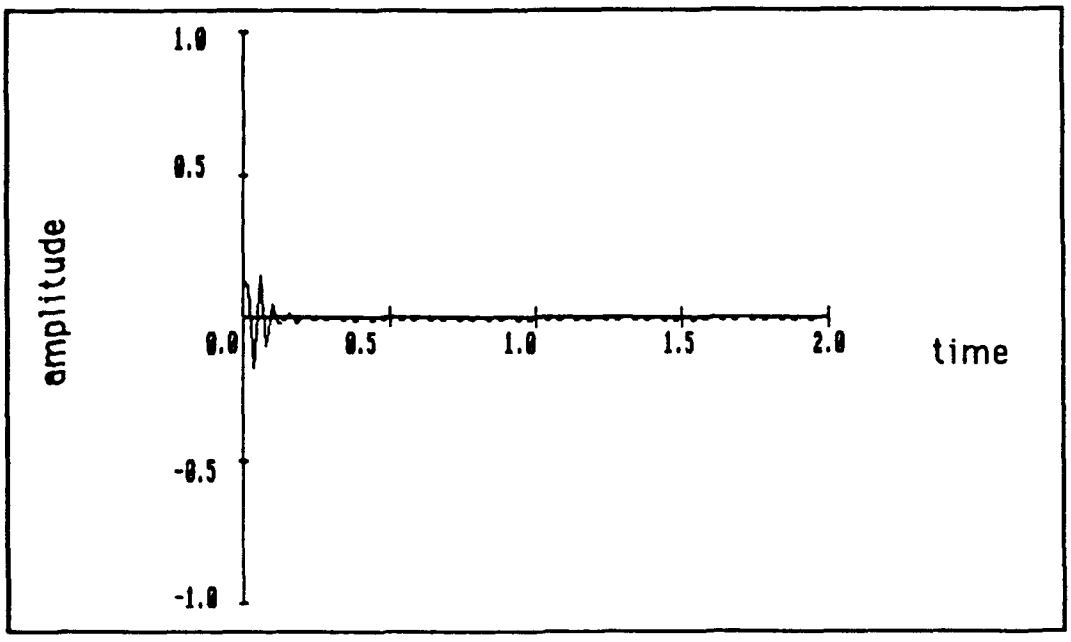

e) 1000 levels in, 1000 levels out

Figure 4.1.2 (cont'd) The effect of limited numerical resolution

4.2 The effect of SLM light leakage

In section 2.3.2 we showed that spatial filtering could significantly reduce the amount of light leakage that is due to transparent space between the pixels of the SLM. In this section we examine just how much of a problem light leakage can be, with regard to overall system performance. Since light leakage can also occur due to light passing through "opaque" off pixels that aren't quite opaque, spatial filtering may not eliminate all light leakage. As we shall see in this section, it is an effect that should not be ignored when evaluating system performance.

Light leaking through the transparent space between pixels, or through "off" pixels due to imperfect polarization, is summed in the vertical direction by the cylindrical lens. This gives nonzero light levels all across the spatial light pattern, thus having the effect of assigning nonzero values to all weight components, regardless of what the microprocessor computes.

The effect of this on overall system performance was simulated on a computer. The same program and noise cancellation problem as were used in obtaining the examples of section 4.1 were used here. The program logic was modified to include the effect of an optical noise level on the output weights, as follows:

```
if output_weight [i] < noise_level then
    output_weight [i] := noise_level.
```

Only the output weight values were affected. The values of the stored weights, to be used on the next iteration, were not corrupted. This accurately reflects what would happen in our hybrid system, since the weight values are stored in the microprocessor. This is fortunate, otherwise the effect of light leakage would be additive on every iteration.

The simulation results are shown in figures 4.2.1 (a) and (b). This example included limited accuracy effects of 256 levels on input and 100 levels on output, as in the example of figure 4.1.2 (d). Figure 4.2.1 (a) shows the effect of an optical noise level of 0.01 (ie., 1 per cent of the maximum weight value). The system performance is virtually the same as that shown in figure 4.1.2 (d). This indicates that the system can handle this amount of light leakage without any further degradation in performance than what is already occurring due to limited accuracy effects. However, if the optical noise level is allowed to reach 0.05 (5 per cent of the maximum weight value), system performance is drastically affected, as shown in figure 4.2.1 (b).

These simulation results show that the effects of light leakage can be significant, and should be considered as a source of system performance degradation, if that performance does not meet expectations.

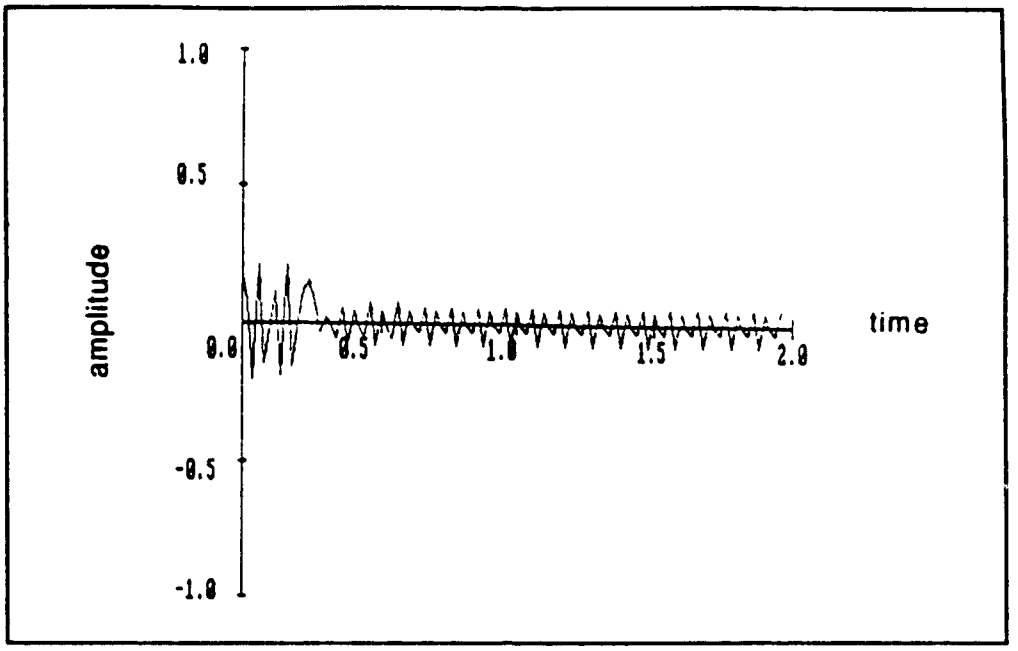

a) 1 per cent light leakage

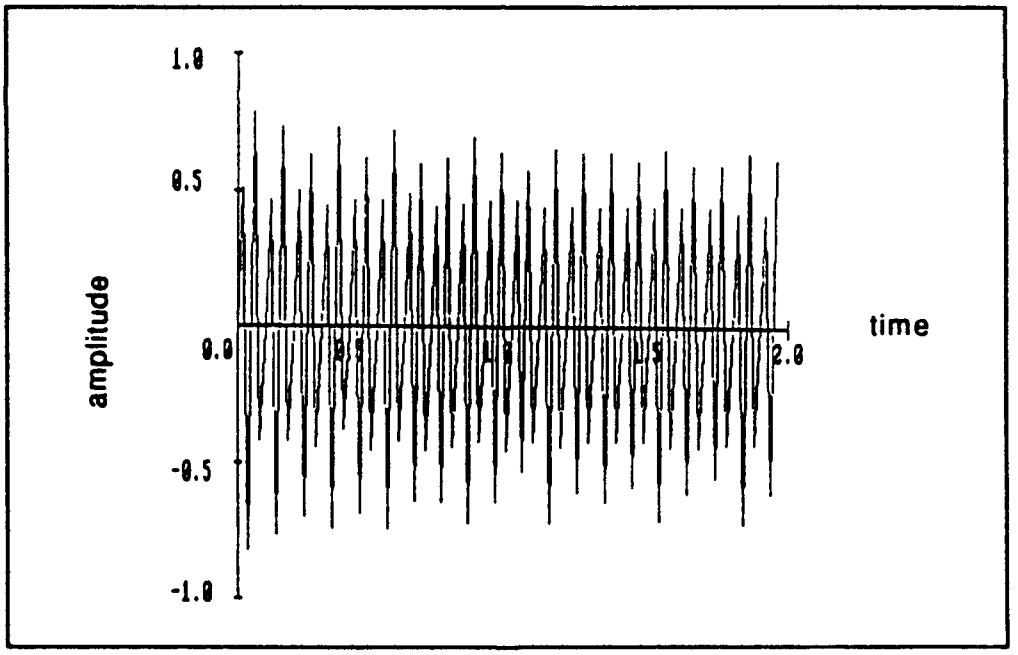

b) 5 per cent light leakage

Figure 4.2.1 The effect of light leakage

4.3 Using the microprocessor to vary the stepsize

As part of the research for this project, a new way of dynamically varying the algorithm stepsize was discovered. The usual method of computing an optimum variable stepsize for the steepest descent and similar algorithms involves specific knowledge of the equation being solved that we do not have available. The new method developed here uses only information that we do have available. We show that it can significantly improve performance.

Consider the usual form of the variable stepsize steepest descent algorithm:

$$w_{n+1} = w_n + a_n r_n$$
$$r_n = b - Aw_n.$$

The iterates w_n converge to the solution of the linear equation

$$Aw = b.$$

The optimum choice of the stepsize a_n is known to be

$$a_n = (r_n, r_n) / (r_n, Ar_n). \tag{4.3.1}$$

Computation of this quantity requires specific knowledge of A and b, in order to compute Ar_n. At this point in our processor, we don't have A and b. What we have available is w_n, r_n, a_{n-1} (ie., whatever was used on the last iteration as a stepsize), and we can remember information from previous iterations, such as w_{n-1}, r_{n-1}, etc.

Note that

$$\begin{aligned} r_{n-1} - r_n &= (b - Aw_{n-1}) - (b - Aw_n) \\ &= A(w_n - w_{n-1}) \\ &= a_{n-1} A r_{n-1}. \end{aligned}$$

Thus,

$$a_{n-1}[(r_{n-1}, r_{n-1}) / (r_{n-1}, r_{n-1} - r_n)] = (r_{n-1}, r_{n-1}) / (r_{n-1}, Ar_{n-1}). \tag{4.3.2}$$

Note that the quantity on the right has the same form as the right side of (4.3.1), although the subscripts indicate the previous iteration. We have available all of the quantities on the left side of (4.3.2), hence we can compute the quantity on the right side of this equation. Thus it might be fruitful to define our stepsize iteratively in terms of the left side of (4.3.2), that is we define a_n as

$$a_n = a_{n-1}[(r_{n-1}, r_{n-1}) / (r_{n-1}, r_{n-1} - r_n)]. \tag{4.3.3}$$

Here, r_n is just the weight update vector that is input to the microprocessor, and a_{n-1} is the stepsize used on the previous iteration. Evaluation of (4.3.3) thus requires storage of the previous weight update vector (r_{n-1}) and stepsize, and the computation of two vector dot products and a scalar division.

Equation (4.3.3) does not yield an optimum stepsize, since that is given by (4.3.1). In fact, (4.3.3) gives us the optimum stepsize one iteration "late". However, when the convergence process nears the correct solution, there won't be much change in the stepsize from one iteration to the next, and (4.3.3) can be viewed as a way of intelligently choosing an appropriately small stepsize. In practice, (4.3.3) should be used in conjunction with a fixed maximum stepsize. If (4.3.3) yields a value larger than this fixed maximum, then the maximum value is used, otherwise, the value from (4.3.3) is used.

This variable stepsize algorithm was incorporated in to the simulation program used in the previous sections. When applied to the same scenario as that used for figure 4.1.2 (d), the system performance improved from 22 dB of cancellation to 29 dB. Moreover, this level of performance was achieved with fewer iterations.

This variable stepsize algorithm can be incorporated into the existing design with no additional hardware cost. The computational cost may prove to be a burden in terms of real time performance, particularly since it is dependent upon the number of weight vector components. However, this should be weighed against the fact that variable stepsize will probably result in fewer iterations, better performance, and may be essential in enabling the system to respond to changing signal scenarios.

5. CONCLUDING REMARKS AND RECOMMENDATIONS

5.1 Conclusion

The hybrid electro-optic processor has been taken from concept to partial fabrication and preliminary testing during the course of this project. The test results of section 3 have shown that an optically generated signal can be used to match, and thus cancel, an electronic signal. We have found a way to overcome the limited dynamic range of currently available spatial light modulators. Simulation results show that our present design should be capable of nearly 30 dB of cancellation performance.

As a follow on effort, we hope to complete construction and testing of this processor, and continue to research ways of improving its performance. In the following sections we discuss some things to keep in mind during the course of future work on this processor.

5.2 Recommendations

5.2.1 SLM technology

Spatial light modulation is a key aspect of the operation of this processor, and we have not as yet demonstrated that currently available devices meet our needs. We should keep abreast of developing SLM technology, and compare new device characteristics against the check list of desired properties given section 2.4.

It is the feeling of this author that the most promising near term technology is liquid crystal displays. Fortunately, this is currently an active research area thanks to the influence of high definition television (HDTV) and its need for flat panel displays. While our needs do not exactly coincide with HDTV's, nevertheless we should keep aware of the continuing new developments in this field.

Active matrix electronic drive technology for liquid crystal displays is one HDTV spinoff that we might be able to make use of. This technology provides each pixel with its own electronic addressing, so that individual pixels can be turned on and off, without having to reset entire rows at a time. This should eliminate the oscillation problems that we encountered with our video addressed LCTV.

Ferro-electric liquid crystals, discussed in section 2.4, also appear to hold promise. Since each pixel holds its on/off state until switched, this type of liquid crystal should also be free of oscillation problems. This property should also eliminate the need for an active matrix driver. There are small (10X10 pixels) active matrix ferro-electric liquid crystal modulators available, as well as larger (128X128 pixels) line addressed modulators.

Another conceivable means of achieving one dimensional spatial light modulation is to use a row of light sources, such as light emitting diodes (LED's) or laser diodes. This is

indeed a possibility, however this approach is not without its problems. First of all, we need a continuous bar of spatially modulated light, so there is the problem of physical spacing between the light sources. This is likely to be less of a problem with LED's. However, the noncoherence of the LED light may cause difficulties when interacting with an ADM, since the ADM will separate the light into its different wavelengths in the first order. We also require high dynamic range from each light source (unless a two dimensional array is used in conjunction with a cylindrical lens in a configuration similar to what we now have) and uniform linear response from all the light sources. Finally, at least in the case of laser diodes, one must consider the cost of putting together 100 or more light sources with independent drivers.

Nevertheless, we should keep an eye on LED/laser diode technology with this application in mind. This approach is particularly important to keep in mind if it is ever desired to implement this processor with integrated optics technology.

5.2.2 Specialized electronics

This is a hybrid system, where we have have attempted to join the advantages of optics and electronics together. The electronic aspect of the processor allows us to precisely implement the iterative algorithm discussed in section 2.1. However, the electronics can also be viewed as a potential bottleneck that may undermine the advantages of the optical processing part of the system. For this reason, the final form of the processor may require specialized electronics to relieve some of the burden from the PC in order to achieve real time operation.

Such electronics would of course include the driver for the SLM, such as the active matrix driver for liquid crystal displays discussed above. Also, specialized electronics could be developed that would incorporate the logic for writing weight patterns on the SLM display, since this is really just a simple addressing operation. This has the advantage of bypassing the graphics of the PC and relieving a tremendous load from the PC processing.

5.2.3 Future enhancements

As part of the follow on effort, we will look at possible enhancements of the system. The most significant near term enhancement would be the expansion to a multichannel system. Multichannel means that the processor could receive inputs from multiple auxiliary omni antennas. Thus, instead of just $n_1(t)$, we would have also $n_2(t)$, $n_3(t)$,...,etc. There is still just a single main antenna input d(t), and the processor produces a single output y(t) to estimate the total jamming single n(t) received at the main antenna. We will look at ways of incorporating multichannel acousto-optic cells into possible multichannel architectures. The anticipated challenges of implementing such an architecture are in the areas of data acquisition and spatial light modulation.

REFERENCES

1. S.T. Welstead, "Implementation of iterative algorithms for an optical signal processor," RL Technical Report TR-88-175 (1988.)

2. V.C. Vannicola and W.A. Penn, "Acousto-optic adaptive processing," GOMAC Digest of Papers, Vol. X, pp 404-409 (1984.)

3. D. Blanchard and M. Ward, "Characterization of liquid crystal displays for signal processing applications," RL Technical Report TR-89-226 (1989.)

4. D.A. Gregory, "Real time pattern recognition using a modified liquid crystal television in a coherent optical correlator," Appl. Opt., Vol. 25, No. 4, pp 467-469 (1986.)

PUBLICATIONS, PATENTS, AND PRESENTATIONS

The following publications, patent applications, and presentations were completed during the course of this project:

Publications

S. Welstead, M. Ward, D. Blanchard, G. Brost, S. Halby, "Adaptive signal processing using a liquid crystal television," SPIE Proc., Vol. 1154, pp 244-252 (1989.)

D. Blanchard and M. Ward, "Characterization of liquid crystal displays for optical signal processing applications," RL Technical Report TR-89-226 (1989.)

Patent Application

S. Welstead and M. Ward, "Extended dynamic range 1-D spatial light modulator," as described in section 2.5 of this report, patent pending at the U.S. Patent Office (1989).

Presentation

M. Ward, "Adaptive signal processing using a liquid crystal television," presented at the SPIE International Technical Symposium on Optoelectronic Engineering, Real Time Signal Processing XII, San Diego (1989.)

MISSION

OF

ROME LABORATORY

Rome Laboratory plans and executes an interdisciplinary program in research, development, test, and technology transition in support of Air Force Command, Control, Communications and Intelligence (C^3I) activities for all Air Force platforms. It also executes selected acquisition programs in several areas of expertise. Technical and engineering support within areas of competence is provided to ESD Program Offices (POs) and other ESD elements to perform effective acquisition of C^3I systems. In addition, Rome Laboratory's technology supports other AFSC Product Divisions, the Air Force user community, and other DOD and non-DOD agencies. Rome Laboratory maintains technical competence and research programs in areas including, but not limited to, communications, command and control, battle management, intelligence information processing, computational sciences and software producibility, wide area surveillance/sensors, signal processing, solid state sciences, photonics, electromagnetic technology, superconductivity, and electronic reliability/maintainability and testability.